






Review

Dripping Rainfall Simulators for Soil Research—Performance Review

Vukašin Rončević ^{1,*} , Nikola Živanović ² , John H. van Boxel ³ , Thomas Iserloh ⁴  and Snežana Štrbac ¹ ¹ Institute of Chemistry, Technology and Metallurgy, University of Belgrade, Njegoševa 12, 11000 Belgrade, Serbia² Faculty of Forestry, University of Belgrade, Kneza Višeslava 1, 11000 Belgrade, Serbia³ Institute for Biodiversity and Ecosystem Dynamics (IBED), University of Amsterdam, Science Park 904, 1098 XH Amsterdam, The Netherlands⁴ Department of Physical Geography, Trier University, Universitätsring 15, 54296 Trier, Germany

* Correspondence: vukasin.roncevic@ihtm.bg.ac.rs

Abstract: Rainfall simulators represent often-used equipment for soil research. Depending on their performance, they could be appropriate for some soil research or not. The aim of this research is to provide insight into the capabilities of existing dripping rainfall simulators (DRS) to mimic natural rainfall and the frequency of simulated rainfalls of certain characteristics, facilitate the selection of rain simulators that would best meet the needs of soil research and to reach a step closer to the standardization of rainfall simulators. DRS performance was analyzed integrally, for simulators with more than one dripper (DRS_{>1}) and with one dripper (DRS₌₁). A statistical analysis was performed for the performance of the DRS, wetted area, drop size, rainfall intensity, duration and kinetic energy. The analysis showed that DRS can provide rainfall that corresponds to natural rainfall, except in terms of the drop size distribution and wetted area. However, usually there are more factors that do not correspond to natural rainfall, such as the median drop size, volume and kinetic energy. Metal and plastic tubes (MT and PT) as the most present dripper types showed a strong relation between the outer diameter (OD) and drop size, while the inner diameter (ID) relation was moderate-to-weak. However, when increasing the range of MT drippers, for diameter size, the relation significance becomes very strong for bouts ID and OD. With the increase in the ID of PT, the relation deviates from the logarithmic curve that represents all drippers together. The sizes of the drops generated by the drippers are mostly in the range between 2 and 6 mm, while the number of drops smaller than 2 mm is relatively small. The intensity and duration of the simulated rain can be successfully produced to match natural values, with the most frequently simulated short-term rainfall of a high intensity. Most simulations were conducted at a fall height of up to 2 m, and then their number gradually decreases as the height gets closer to 5 m. Most simulations (58.6%) occur in the range between 20–90% KE, then 33.0% in a range of 90–100%, with only 8.4% lower than 20% KE.

Keywords: dripping rainfall simulators; drippers; simulator performance; soil research; rainfall simulator review



Citation: Rončević, V.; Živanović, N.; van Boxel, J.H.; Iserloh, T.; Štrbac, S. Dripping Rainfall Simulators for Soil Research—Performance Review. *Water* **2023**, *15*, 1314. <https://doi.org/10.3390/w15071314>

Academic Editor: Maria Mimikou

Received: 18 January 2023

Revised: 8 March 2023

Accepted: 21 March 2023

Published: 27 March 2023



Copyright: © 2023 by the authors. Licensee MDPI, Basel, Switzerland. This article is an open access article distributed under the terms and conditions of the Creative Commons Attribution (CC BY) license (<https://creativecommons.org/licenses/by/4.0/>).

1. Introduction

Rainfall simulators represent often-used equipment for soil research. According to the process of the formation of water drops, rainfall simulators can be divided into simulators that generate drops by spraying (Spraying Rainfall Simulators—SRS) [1–5] and by dripping (Dripping Rainfall Simulators—DRS) [6–9]. In addition to the mentioned groups, there is also a group of simulators that generate drops using the combined action of the two processes (Combined Rainfall Simulators—CRS). They usually involve nozzles or drippers that primarily create precipitation and different metal meshes, modifying the precipitation. They are created in an attempt to compensate for the shortcomings of simulators from the two previously mentioned groups [10–15]. Rainfall factors that are

significant in terms of their impact on soil are the amount, intensity, duration and regime of precipitation [16–19], distribution raindrop sizes [20–22], spatial distribution [23], raindrop size, falling speed [24,25], direction of fall [26,27], direction of movement [18], kinetic energy [28], momentum [29] temperature [30] and chemical composition of rainfall [31].

It is important to keep in mind that simulator design and performance are mutually conditional, so to understand the simulator design it is necessary to analyze their performance as well [32]. By analyzing the rainfall simulators and comparing them with each other, the main differences in their performance were noted. SRS provides a distribution of water drop sizes that is more similar to natural precipitation, enables the establishment of the terminal velocity of the drops at a lower height and is advantageous in terms of the ease of manufacture, portability, the surface they can cover, handling and the price of the simulator [33,34]. On the other hand, DRS generate precipitation in a wider range of intensity, with the possibility of changing the intensity of precipitation without a significant change in the size of the drops and achieving greater uniformity of the spatial distribution of precipitation [9,34–36]. Simulators with only one dripper, by their design, enable a special analytical approach in the study of soil with the individual erosive action of drops on the soil [22,37–42].

Different research criteria and available resources have led to the development of simulators of specific design and performance [6,12,35,43–50].

Until now, several studies have been carried out in which rain simulators were presented, classified, and analyzed, in which their design was described, and some of their performances and areas of use were presented [34,51–55]. However, even though individual characteristics of the simulator and the general characteristics of the groups to which they belong are presented, a comparative analysis of the simulator performance factors is missing. Analysis of the individual performance of a relatively small number of simulators were provided by [55], while [56] conducted a detailed comparative analysis of the performance of 13 small portable rain simulators, of which two types are DRS, while the others are SRS.

The aim of this research is to review performances of DRS and CRS in which, during the primary phase, precipitation is created only by drippers. This research should provide insight into the capabilities of simulators to mimic natural rainfall and the frequency of simulated rainfalls of certain characteristics, facilitate the selection of rain simulators that would best meet the needs of soil research and reach a step closer to the standardization of rainfall simulators.

2. Materials and Methods

Due to the large number of data and the required extensive analysis, only the performance of DRS was analyzed in the research. ResearchGate, Google Scholar, KoBSON, COBISS, Academia.edu, JSTOR and Scopus internet databases of scientific works were used during the research. A search was conducted for all available scientific papers describing DRS and papers that include a wide range of thematically related papers to soil research in which DRS are used starting from 1941 until today. Together with the performance of DRS, this analysis has also included the performance of CRS in which, during the primary phase, precipitation is created only by drippers.

In order to analyze the performance of DRS, descriptive and numerical data sorted by category for each type and subtype of the simulator [32] were extracted from the papers, namely: surface and shape of the wet area of the plot, Christiansen's coefficient of uniformity of spatial distribution of precipitation, intensity and duration of simulated precipitation, diameter, the height of fall and kinetic energy of the generated drops.

In addition to the aforementioned categories of data, we also analyzed the data on the origin and temperature of the water used during the simulations, because these are also important factors.

The analysis of the performance of the rainfall simulator was carried out integrally for simulators with one dripper ($DRS_{=1}$) and more than one dripper ($DRS_{>1}$). However,

$DRS_{=1}$ was not used in the analysis of the distance between the drippers, the surface and the shape of the wetted area of the plot, the Christiansen coefficient of uniformity of spatial distribution of precipitation and the intensity of the precipitation. The performance analysis of the simulator, i.e., the factors of simulated rainfall, includes a descriptive and relational statistical analysis of the numerical values of the factors and the agreement of those values with the values of the factors of natural rainfall. Droplet kinetic energy was determined from the fall height and drop diameter data using the [57] numerical model for determining the raindrop terminal and achieved velocity.

The types and subtypes of simulators, whose performance was analyzed, were separated and presented in the work of [32]. Considering that not all the data according to the separated categories were available for every type or subtype of the simulator, an independent comparative analysis of the available data was carried out within categories.

The collected data were classified and presented using the LibreOffice 4.4 software package. Additionally, statistical data analysis was performed using LibreOffice 4.4 and IBM SPSS Statistics 20 software packages.

3. Results and Discussion

Out of a total of 188 scientific papers included in the analysis, 51 different types and 27 subtypes of $DRS_{>1}$ were singled out in 149 papers (Table S1 in Supplementary Materials), and in the remaining 39 papers, as many as 25 different types and 4 subtypes of $DRS_{=1}$ (Table S2) [32].

3.1. Wetted Area

The wetted area of $DRS_{>1}$ represents the surface of the experimental plot that is exposed to simulated rainfall. The shape is most often rectangular but can also be round, and its dimensions are determined by the shape and dimensions of the projected drippers surface [7,58–61].

In the analysis, two sets of data were combined: the exact and approximate wetted area. The first set represents explicitly stated values of the area or dimensions of the wetted area. The second dataset represents the wetted area data based on the assumption that the dimensions or a covered area of the water tank with drippers above correspond to the dimensions and area of the wetted area below. The second dataset gives values that are usually slightly overestimated; however, for a general analysis, this can be neglected.

The largest number of simulators covers a wetted area between 0.2 and 0.6 m² (Figure 1). A smaller number of simulators have a wet surface area below 0.2 m² and in the range of 0.8–1.0 m², while the number of simulators with a wetted area larger than 1.0 m² is significantly lower. One rainfall simulator had a wetted area of 36 m² [9]. Wetted areas covered by rain simulators of a modular design were not included in the analysis, but only the wetted areas were covered by separate modules.

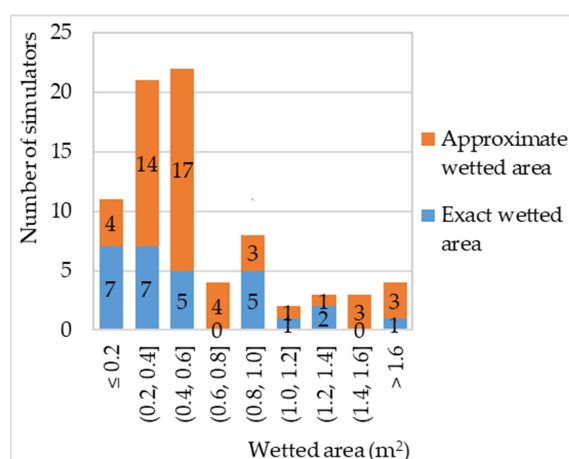


Figure 1. The number of DRS simulators with different wetted surface sizes.

3.2. Drop Size

Natural or simulated rainfall drop size is defined by the diameter of a sphere whose volume is identical to the drop volume, although raindrop shape usually is not entirely spherical [62–64]. The choice of drippers for the DRS is often based on the experience of previous research or personal empirical knowledge, under the assumption that drippers in the form of tubes and holes with a smaller internal diameter (ID) generate drops of a smaller diameter and vice versa, neglecting other factors that affect the size of the drops. However, when fitting logarithmic functions, the dripper diameter of metal and plastic tubes (MT and PT) showed a strong relation for the dripper's outer diameter (OD), while the relation for the dripper's ID is moderate-to-weak (Figure 2a,b). For some of the drippers, both the ID and OD values were available, so their pairs can be noticed on the graphic.

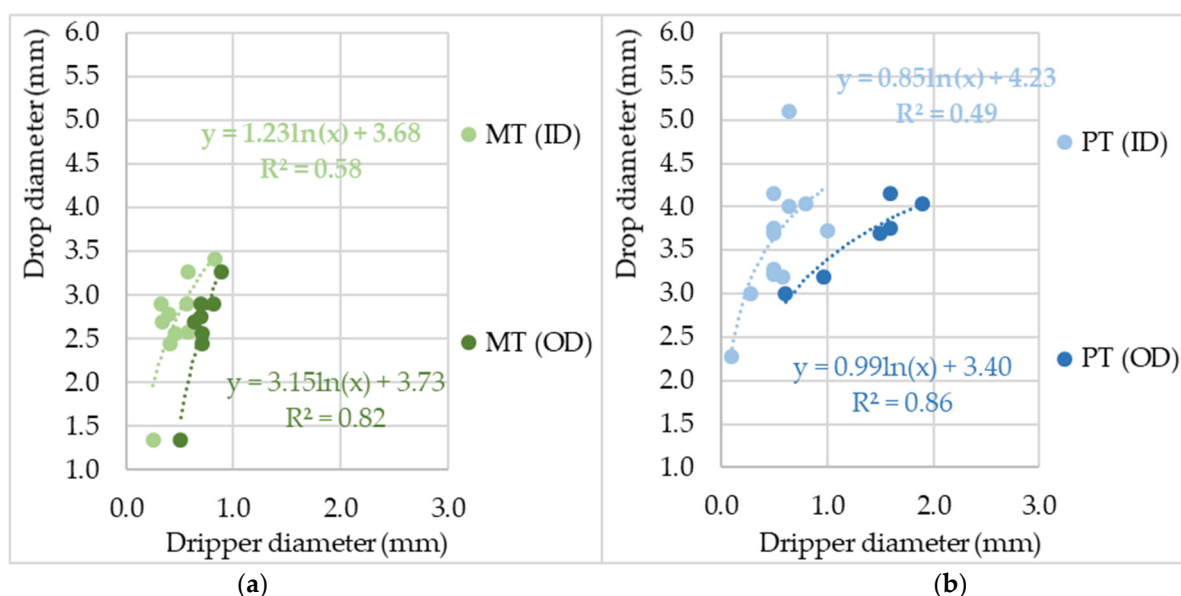


Figure 2. The influence of MT (a) and PT (b) drippers OD and ID on the drop diameter. Note: drippers whose corresponding drop diameter sizes were modified by the action of air, vibrations and inserted threads, and drops and drippers whose diameters were given in a range, were excluded from the analysis.

However, when increasing the range of the MT drippers' diameter size the relation becomes very strong, $R^2 = 0.96$ and 0.97 , for both the ID and OD. Additionally, the logarithmic function that describes that relation is in accordance with data obtained by [65], where water drops were generated using hypodermic needles (Figure 3). On the other hand, observations by [66] showed that as the dripper diameter increased, the detached drop weight became less dependent on the dripper diameter.

In general, the relation between drippers and drop diameter, described using the logarithmic equation, shows a very strong relation for the dripper's OD, and a weaker but still strong relation for the ID (Figure 4). That is in accordance with [12], who roughly estimated that at the same water pressure, the OD size of the dripper determines the size of the drop.

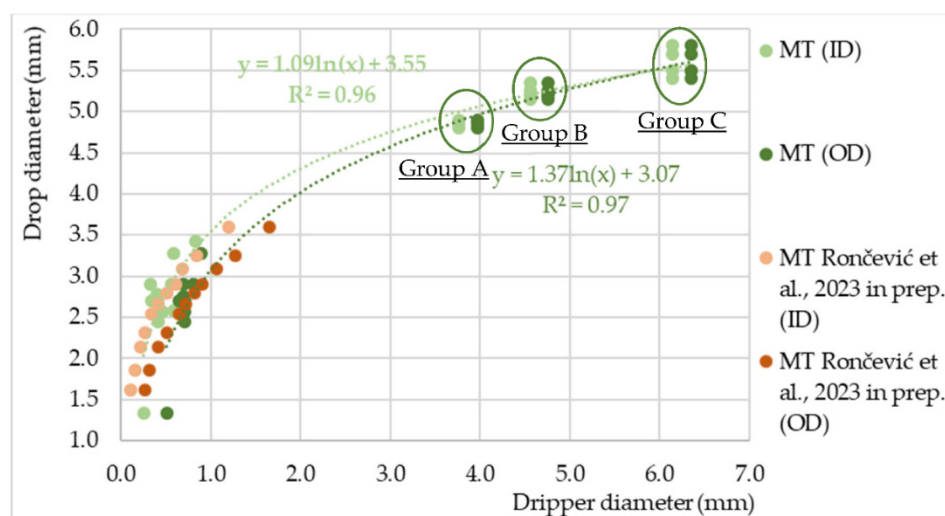


Figure 3. The influence of MT and PT drippers' ID and OD size on the drop's diameter with expanded diameter range (groups A, B and C) of MT drippers [67] in comparison to research of [65] Note: drippers whose corresponding drop diameters size were modified by the action of air, vibrations and inserted threads, and drops and drippers for which the diameter was given in a range, were excluded from the analysis. The equations shown exclude the data from the research of [65].

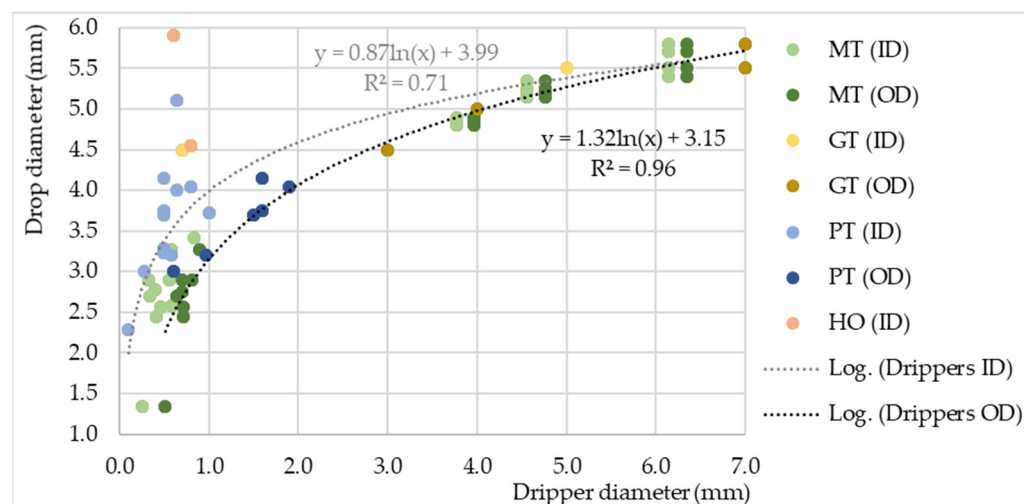


Figure 4. The influence of different types of drippers' ID and OD on drop diameter size (GT—glass tubes, and HO—holes in boards and tubes). Note: drippers whose corresponding drops diameter size were modified by the action of air, vibrations and inserted threads, and drop and dripper diameters given in a range, were excluded from the analysis.

It is obvious that with the increase in the ID of the plastic tubes, the relation deviates from the logarithmic curve that represents all drippers together. Additionally, there are HO drippers whose values deviate from the logarithmic curve too, but they are specific because they have an almost infinite outer diameter (Figure 4). It is suggested that a possible reason for such a deviation could be the dripper material. However, based on the research of [68–72], drippers made from different materials such as glass, brass, stainless steel, Teflon, all show no significant difference in drop size. The material type rather determines the thickness of the tube wall. Metal tube drippers generally have a thinner wall than plastic or glass tube drippers. Based on the data of drippers that had given both an ID and OD size, the thickness of different type tube walls was, respectively, <0.31, 0.33–1.10 and 2.00–2.30 mm. Depending on the geometry of the dripper tip, the drops are formed either at the ID (tubes with sharp, conical tip) or at the OD of the tip (blunt, flat tip) [72–75]. Therefore, when describing the relation between the dripper diameter and drop size, the

assumption is that metal tube drippers have a different logarithmic distribution than plastic or glass tubes, because of their thinner wall (Figure 2a,b and Figure 4), regardless of whether they are sharp or blunt.

However, drop size is not exclusively correlated with dripper diameter, surface tension or dripper tip geometry. The size of the drop depends on numerous other factors; among them are dripping intensity, dripping tip position and geometry, length-to-diameter ratio, water temperature and environmental atmosphere condition [67,72,76].

In addition to the dripper diameter and type, the dripping speed is also a factor that was taken into account for soil research using rainfall simulators. [25]. With the rise in the dripping speed, the drop size of the MT drippers rises too, until it starts to decline at some point [65]. Separated data groups A, B and C, which can be seen in Figure 3, represent the research data of [67]. Three MT drippers of different diameters generated drops whose diameters differ due to different dripping intensities and have values of 2, 4, 8 and 12 cm³. Although the dripping intensity difference is quite big, the drop size does not differ much. On the other hand, the difference was larger in the research of [50]. They used PT drippers with an ID of 0.5 mm and an OD value of 1.6 mm, at two different dripping intensities of 160 and 200 mm/h, resulting in drop sizes of 3.75 and 4.15 mm, respectively (Figures 2a,b and 4).

Additionally, the influence of water temperature on the size of the generated drop is significant [76]. Water used in rainfall simulations with DRS can be distilled water [37,39,77,78] or water available from the environment, which is most often water from the water supply network [79–84]. Of the physical characteristics of water, the temperature is most often mentioned [42,85–87], while the chemical composition of water is given in rare cases [63,83,88,89]. Based on the analysis of the recorded water temperature values in the available scientific works, it was determined that its values are predominantly in the range of 5–30 °C, with the most common values recorded in the range of 15–20 °C (Figure 5).

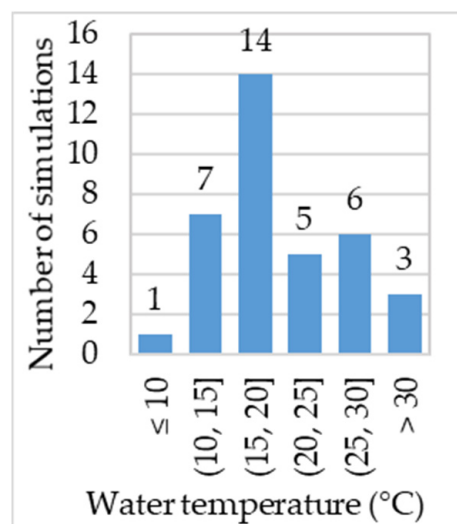


Figure 5. Measured water temperature values during rainfall simulations.

Modifications of dripper performance via air flow and vibration were carried out in order to expand the range of drop sizes, primarily with the aim of also generating drops with smaller diameters [90,91]. Additionally, threads inserted in drippers were applied primarily to achieve capillary movement of water in the dripper and reduce flow, despite the fact that they change the diameter of the generated drop [44,92]. In some cases, drippers in the form of tubes are inserted telescopically into each other (with water flow in a direction from the smaller to larger dripper diameter) in order to form drops corresponding to the ending dripper with the largest internal diameter, with a reduced intensity of dripping, thus facilitating dripping intensity regulation [67,93].

The sizes of the drops generated by the drippers are mostly in the range between 2 and 6 mm, while the number of drops smaller than 2 mm is relatively small (Figure 6). Although it is stated that the diameter of the drops of natural precipitation can reach 6, 7 and even 8 mm, it rarely exceeds 4 mm [94–96]. Falling drops are stable at terminal velocity until they reach a diameter of 4.6 mm, after which they break up into smaller ones due to the air resistance encountered during their fall, becoming definitely unstable with a diameter above 5.5 mm [97]. On the other hand, the maximum value of the median volume diameter (D_0) of natural precipitation is only 2.0–2.5 mm at an intensity of 25–200 mm/h [98], which is in agreement with the observations of other researchers [21,99], whereas higher values have been reported also [100–102]. However, these D_0 values refer most often to rains of a relatively high intensity, while rains of a lower intensity occur more often and achieve relatively lower D_0 values [103]. Accordingly, it is important to determine the method of generating drops with a diameter smaller than 2 mm in order to carry out simulations of rainfall with a smaller diameter. Drops of a larger diameter are successively produced with DRS. Although they occur much less often, they can cause considerable soil erosion.

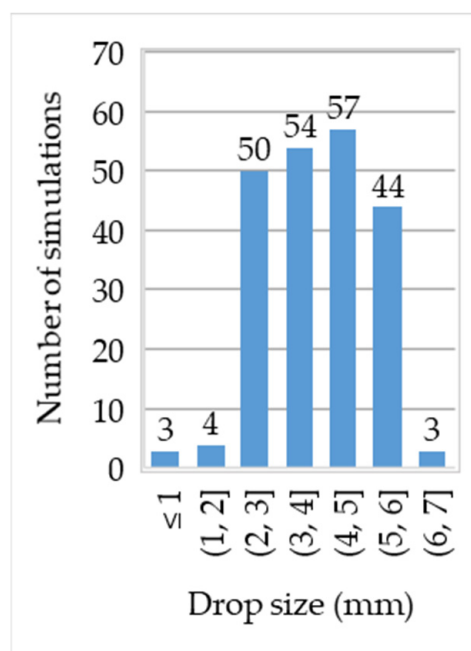


Figure 6. The number of simulations at different sizes of drop diameter. Note: drippers whose corresponding drop diameter sizes were given in a range were excluded from the analysis.

Drippers that generated drops of less than 2 mm dominantly belong to the drippers in the form of metal tubes whose performance is modified by the influence of air flow and vibrations, while the drippers used in the work of [104] generated drops of less than 2 mm with a relatively small dripper diameter, while in the work of [105], the drops were generated using electrical pulse generator technology. [84] did not state how such a small drop diameter was generated. [85] state that the dimensions of the hypodermic needle size 25 G (gauge number represents the standardized size of hypodermic needles) produced a drop with a 1.34-mm diameter. This is not in accordance with the expected diameter values assumed on the basis of the diameter of the drops usually obtained by drippers with gauge numbers 26 and 27, which produce a drop of a relatively bigger diameter [25,80,106]. Additionally, it is not in accordance with the research of [65]. Drops whose diameter is at the upper limit of the size of the drops of natural precipitation are not a problem to generate with drippers (Figure 7).

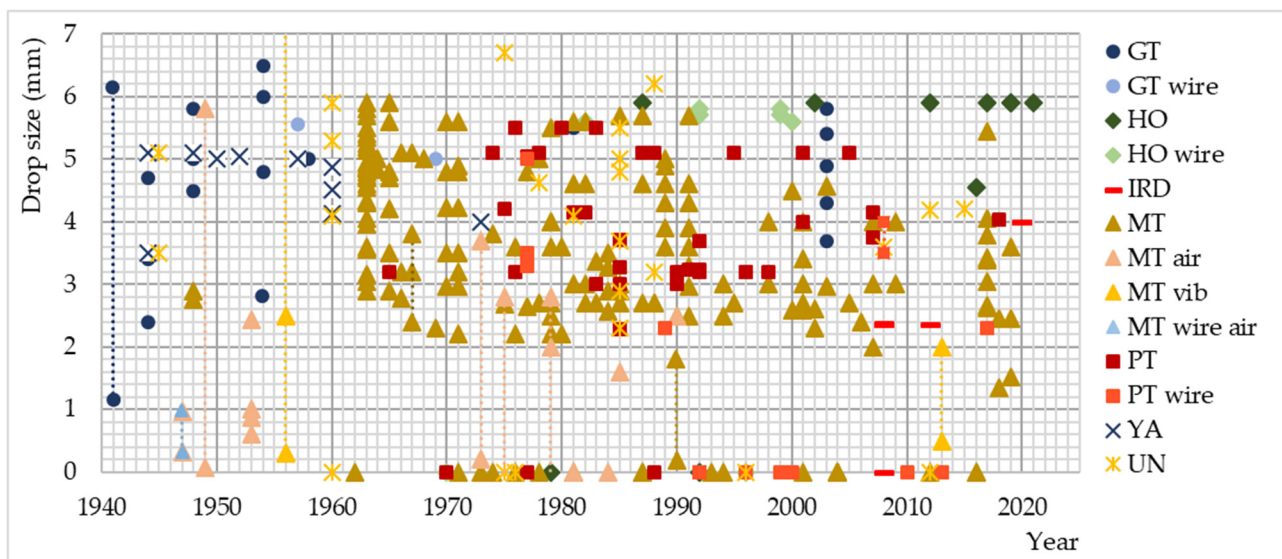


Figure 7. Type and subtype (modified performance drippers) of drippers and corresponding sizes of generated drops used in previous rainfall simulations (GT—glass tubes, GT wire—glass tubes with threads, HO—holes in dripper reservoir, HO wire—holes in dripper reservoir with threads, IRD—irrigation drippers, MT—metal tubes, MT air—metal tubes under the influence of air flow, MT vib—metal tubes under the influence of vibration, MT wire air—metal tubes with threads under the influence of air flow, PT—plastic tubes, PT wire—plastic tubes with threads, YA—hanging yarn and UN—unspecified dripper type). Note: for markers located on a horizontal line with a value of 0, the diameter of the generated drops was not specified [32]. Also, dotted lines represent simulated drop diameter values that are given in a range.

3.3. Rainfall Intensity and Duration

The rainfall intensity of DRS is regulated by regulating the pressure or water flow in the hydraulic system of the simulator [32,107–110].

The most common values of simulated rainfall intensities range up to 50 mm/h, and then their number gradually decreases for the ranges of 50–100 mm/h, 100–150 mm/h and over 150 mm/h, with a maximum value of over 1600 mm/h (Figure 8).

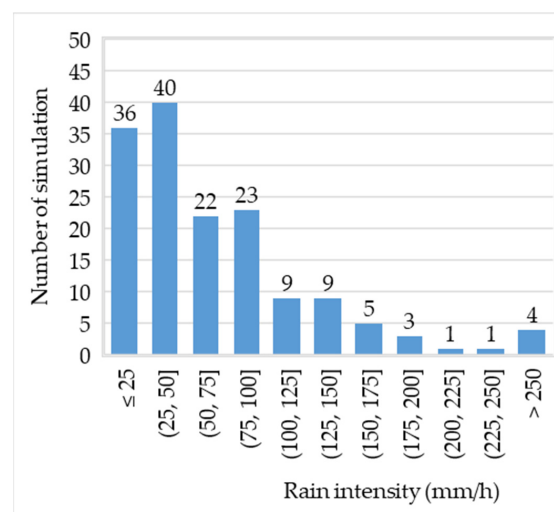


Figure 8. Number of simulations at different intensities of simulated precipitation. Note: simulations with a single dropper or those for which intensity values are given in a range are not included in the analysis.

Rainfall intensity is correlated with drop size median volume (D_0), which, as suggested by [111], is the best parameter for representing the drop size distribution of rainfall. However, the relationship is site specific [112] (Figure 9). With an increase in the intensity of precipitation, the value of D_0 also increases [101,111,113–116]. However, some researchers state that after reaching a rainfall intensity of about 70–100 mm/h, the D_0 hardly changes and stabilizes [98,103,117–120], while some even report that the D_0 decreases [103,121–123] (Figure 9).

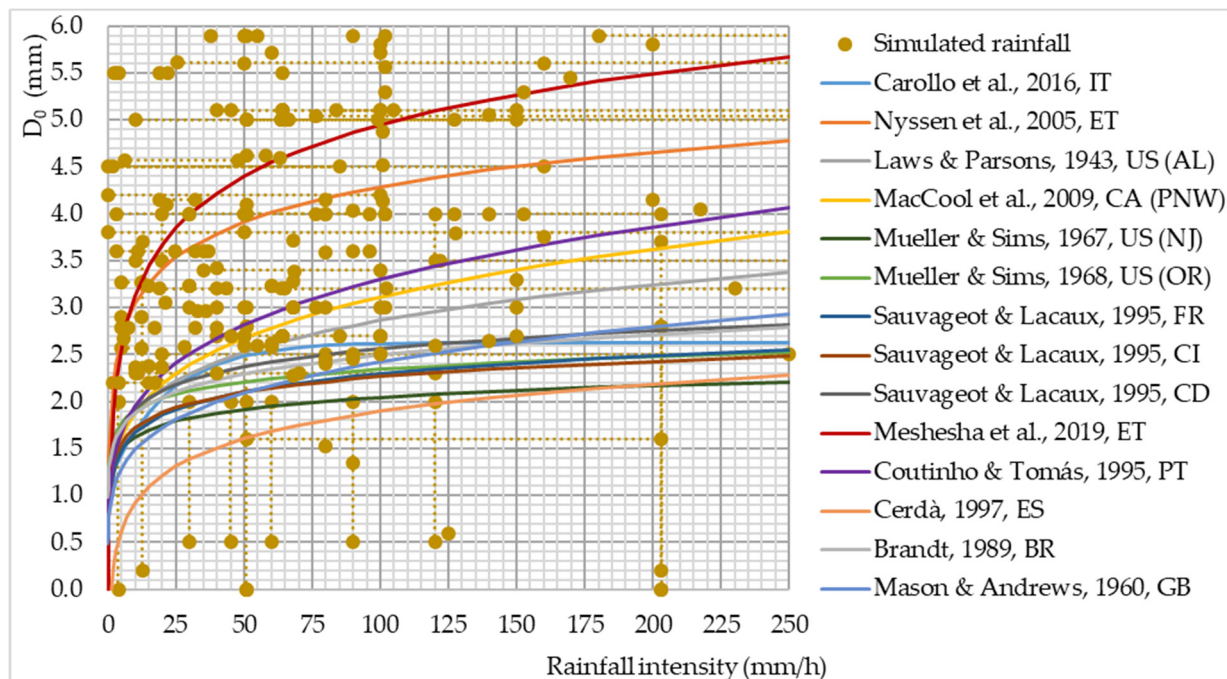


Figure 9. D_0 as a function of intensity for natural and simulated rainfalls. Note: two capital letters after reference represent the ISO Alpha-2 country code that designates countries in which measurements have been conducted [21,54,99–102,113,124–128]. Note: dotted lines represent simulated D_0 and rainfall intensity values that are given in a range.

Given that $DRS_{>1}$ generate precipitation whose drop size uniformity coefficient is theoretically 100% (in practice it will be somewhat lower), the values of the D_0 should correspond to the diameter of any such generated drop. Although it is possible using $DRS_{>1}$ to generate precipitation intensity in the range of the D_0 that occurs in nature, there is a relatively small number of simulated precipitations that corresponds to natural precipitation. D_0 values usually rise until a rainfall intensity between 50–75 mm/h is reached, achieving maximum D_0 values ranging from 2.0–2.7 mm at a precipitation intensity ranging from 75–200 mm/h (Figure 9).

The duration of the simulated rainfall is determined by the availability of water necessary for the simulation and the intensity of the rainfall. If the water necessary for the simulation is available in unlimited quantities, the duration of the simulation is also unlimited, while on the other hand, if the amount of water is limited, the duration of the simulation directly depends on the intensity of precipitation [32]. The largest number of simulations was conducted for a duration of less than 30 min, then the number of simulations gradually decreased to a duration of 2 h, while only a few simulations were conducted for a duration longer than 2 h (Figure 10).

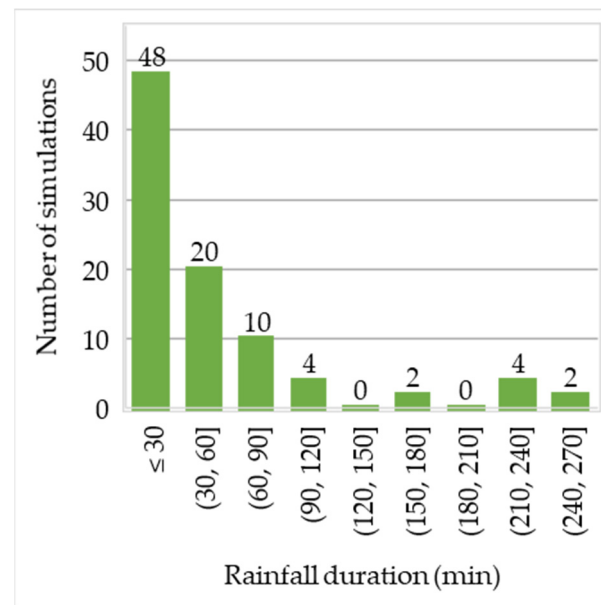


Figure 10. Number of rain simulations at different durations. Note: data whose duration values are given in ranges are not included in the analysis.

In addition to the D_0 , rainfall intensity is also correlated with rainfall duration. The simulated and natural precipitation intensity for the return period of 1–5 years for different geographical areas mostly coincides (Figure 11).

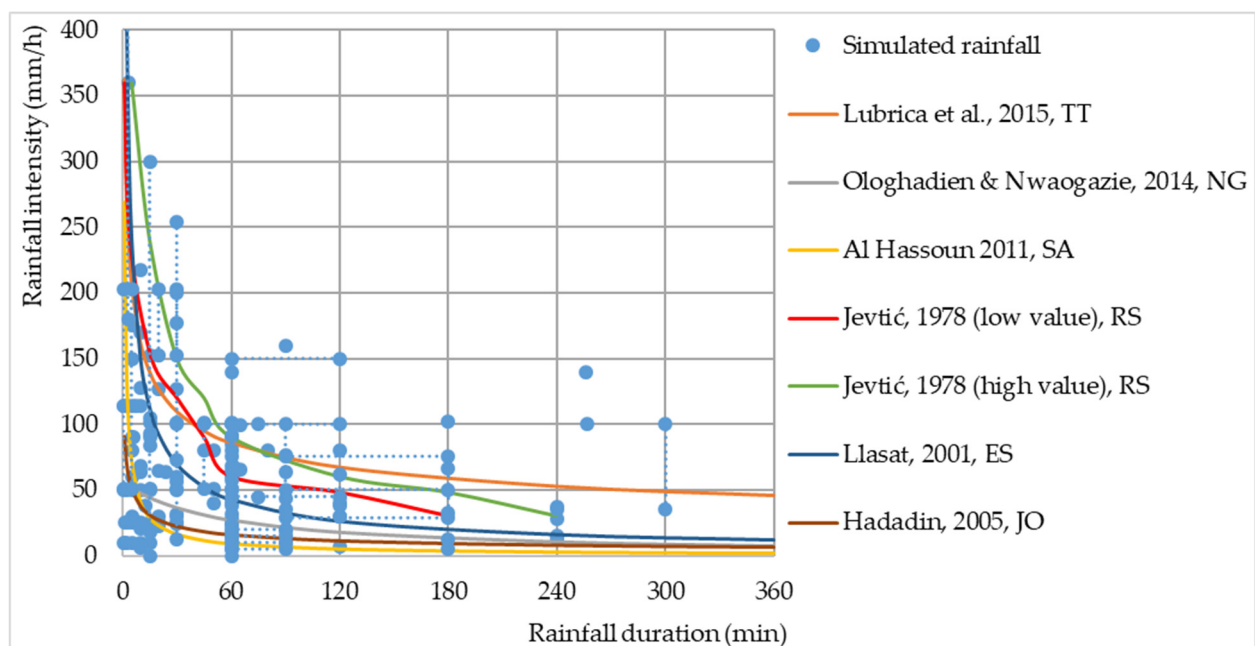


Figure 11. Rainfall intensity as a function of the duration of natural and simulated rainfalls. Note: two capital letters after reference represent the ISO Alpha-2 country code that designates countries in which measurements have been conducted [23,129–133]. Note: dotted lines represent simulated rainfall duration and rainfall intensity values that are given in a range.

3.4. Kinetic Energy (KE)

The KE of rainfall is determined by the size distribution of raindrops and their falling speed. Since the diameter of the drop and the height of the fall are known for $DRS_{>1}$, it is possible to calculate the KE of such precipitation. There are several works that determined the

terminal velocity of drops of different diameters under given conditions [57,104,134–136] however, during simulations, due to the insufficient height at which the drops were placed, terminal velocities were often not reached. Given that the change in drop velocity does not occur linearly with the change in drop height and is different for drops of different diameters, there is no single equation that could represent this relationship [57]. For the purposes of the research, a mathematical model by [57] for determining the terminal and achieving the speed of drops of different diameters at different heights of drops was applied for the determination of the achieved speed, i.e., the KE of drops in the previous simulations (Figure 12).

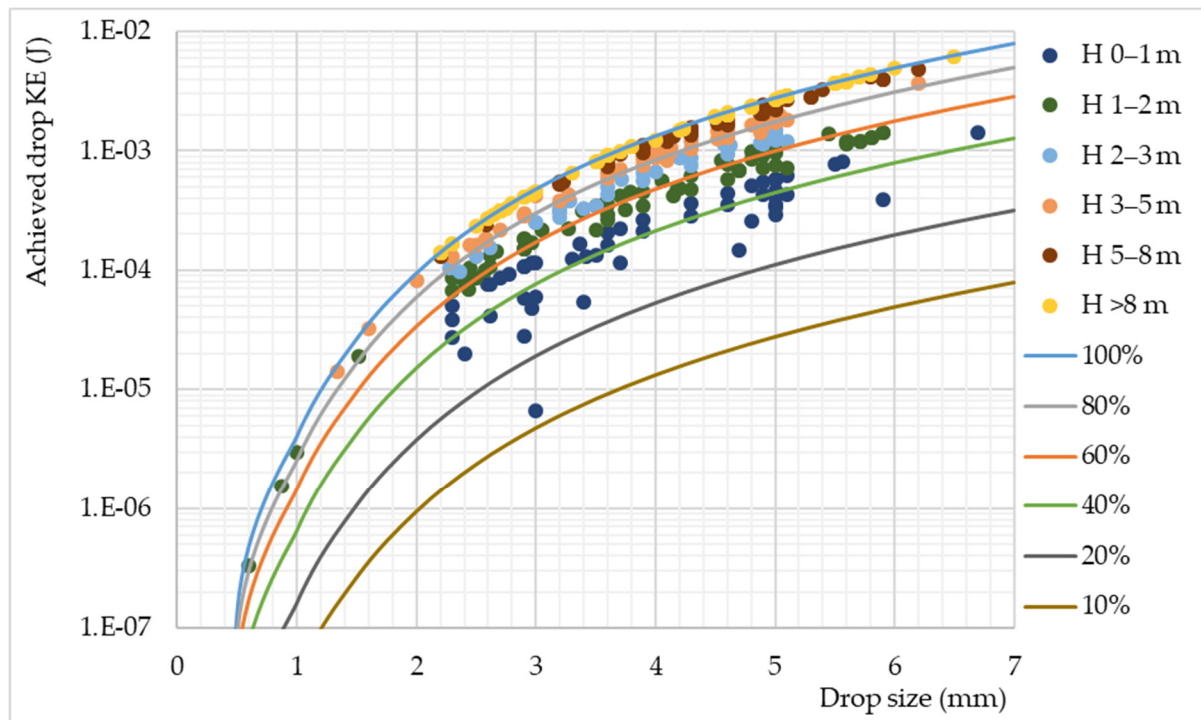


Figure 12. Achieved drop KE of simulated precipitations for different heights based on the mathematical model of [57]. Note: the analysis did not include simulations for which drop height values were given in a range.

For 1-mm drops, the required height to achieve 90% of terminal velocity would be approximately 1.5 m, and for 2-mm drops it would be about 4.0 m, after which it increases to about 5.5 m for bigger drops [57]. Figure 13 shows the representation of different fall heights during the simulations, where it can be seen that most simulations were conducted at a fall height of up to 2 m (43.7%), and then the percentage decreases gradually as the height gets closer to 5 m (31.1%). Falling heights over 5 m occupy 25.2% of all simulations and occur relatively equally, while the highest recorded falling height is 14 m. However, depending on the diameter of the drop, the presented values of the drop height may or may not be satisfactory in terms of achieving the terminal drop speed [57].

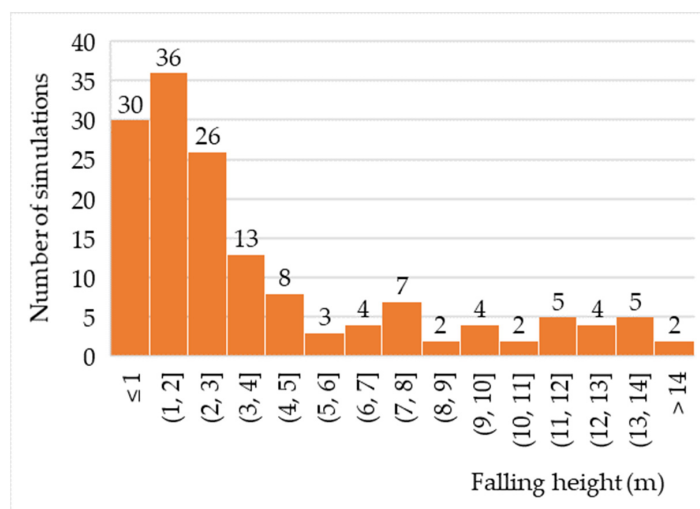


Figure 13. Number of simulations at different heights of simulated precipitation [32]. Note: data whose values are given in ranges are not included in the analysis.

The number of simulations with a KE lower than 30% have a steep rise within categories, after which their number slowly falls with the increase in the KE until reaching the category of 90–100%, which comprises 33.0% of simulations. Most the simulations (58.6%) occur in the range between 20 and 90% KE, while only 8.4% are lower than 20% KE. Drops smaller or equal to 2-mm diameter achieved a KE in a range of 60–80% in 28.6% of the simulations, while 71.4% of the simulations achieved over 85% of the KE (Figure 14).

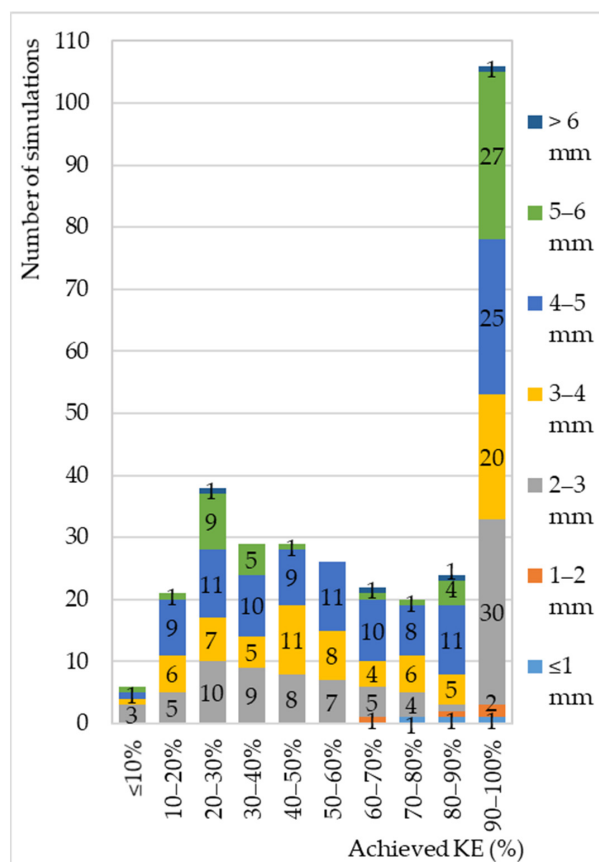


Figure 14. The number of simulations at different values of the achieved KE in relation to falling drops of different diameters. Note: data whose values of drop diameter or fall height are given in ranges are not included in the analysis.

4. Conclusions

The analysis of the performance of DRS determined their ability to properly simulate rainfall. Research showed so far that DRS can provide rainfall that correspond well with natural rainfall, except in terms of the drop size distribution and wetted area, which can be cited as the biggest shortcoming of DRS; on the other hand, usually there are more factors that do not correspond to the natural conditions, such as the median drop size volume and kinetic energy.

The wetted area of most rainfall simulators has a square shape, is relatively small and can be increased by using a modular design simulator.

MT and PT as the most present drippers type showed a strong relation between the OD and drop size, while the ID relation is moderate-to-weak. However, when increasing the range of MT drippers' diameter size, the relation becomes very strong for both the ID and OD. A logarithmic relation between the drop diameter and MT diameter matches very well with the data of [65]. With the increase in the ID of the plastic tubes, the relation deviates from the logarithmic curve that represents all drippers together. It is suggested that a possible reason for such a deviation could be the dripper material. Metal tube drippers generally have a thinner wall than plastic or glass tube drippers. Metal drippers have a different logarithmic relation than plastic or glass tubes because they have a thinner wall.

In addition to the dripper diameter and type, the dripping speed is also a factor that was taken into account for soil research using rainfall simulators. Although the dripping intensity in relation to the MT drippers' difference could be quite high, the drop size does not differ much. On the other hand, the difference was larger for thicker wall tubes.

Water used for simulations is usually distilled water or water available from the environment, which is most often water from the water supply network. The water temperature is predominantly in the range of 5–30 °C, with the most common values recorded in the range of 15–20 °C.

The sizes of the drops generated by the drippers are mostly in the range between 2 and 6 mm, while the number of drops smaller than 2 mm is relatively small. Given that, the maximum value of the median volume diameter (D_0) of natural precipitation is usually only 2.0–2.5 mm, and given that high-intensity precipitation occurs less frequently, it is important to determine the method of generating drops with a diameter smaller than 2 mm in order to carry out simulations of rainfall more similar to natural rainfall. Drippers that generated drops of less than 2 mm dominantly belong to the drippers in the form of metal tubes, whose performance is modified by the influence of air flow and vibrations.

The intensity and duration of the simulated rain can be successfully produced to match natural values, with the most frequently simulated short-term rainfall of a high intensity. The most common values of simulated rainfall intensities range up to 50 mm/h, and then their number gradually decreases for the ranges of 50–100 mm/h, 100–150 mm/h and over 150 mm/h, with a maximum value of over 1600 mm/h. The largest number of simulations was conducted for a duration of less than 30 min, then the number of simulations gradually decreased to a duration of 2 h, while only a few simulations were conducted for a duration longer than 2 h.

Most simulations were conducted at a fall height of up to 2 m, and then the percentage gradually decreases as the height gets closer to 5 m. Falling heights over 5 m occur relatively equally, while the highest recorded falling height is 14 m. However, depending on the diameter of the drop, the presented values of the drop height may or may not be satisfactory in terms of achieving the terminal drop speed.

Most of the simulations (58.6%) occur in the range between 20–90% KE, then 33.0% in the range of 90–100%, and only 8.4% are lower than 20% KE.

Supplementary Materials: The following supporting information can be downloaded at: <https://www.mdpi.com/article/10.3390/w15071314/s1>, Table S1: Classification of DRS_{>1} according to water moving mechanism and water tank with drippers type and shape, with listed literature sources of papers in which simulators are described or applied (W. pump—water pump; CCW—cloth on chicken wire; Not Spec.—not specified; WTD—water tank with drippers). Note: background colors signify different groups in a classification table only to make it easier for reader to observe data. Table S2: DRS₌₁ with the listed sources of papers in which they are described or applied (References [137–261] are cited only in the Supplementary Materials).

Author Contributions: All authors listed have made a substantial intellectual contribution to the work. All authors have read and agreed to the published version of the manuscript.

Funding: This research was funded by the Ministry of Education, Science and Technological Development of Republic of Serbia (Contract No: 451-03-47/2023-01/200026 and Contract No: 451-03-47/2023-01/200169).

Data Availability Statement: The data presented in this study are available on request from the corresponding author.

Acknowledgments: The authors of this paper would like to express their gratitude to the Ministry of Education, Science and Technological Development of Republic of Serbia for realization of this scientific project (registration number 451-03-47/2023-01/200026 and 451-03-47/2023-01/200169).

Conflicts of Interest: The authors declare no conflict of interest.

References

1. Bryan, R.B. An Improved Rainfall Simulator for Use in Erosion Research. *Can. J. Earth Sci.* **1970**, *7*, 1552–1561. [\[CrossRef\]](#)
2. Ogunye, F.O.; Boussabaine, H. Development of a Rainfall Test Rig as an Aid in Soil Block Weathering Assessment. *Constr. Build. Mater.* **2002**, *16*, 173–180. [\[CrossRef\]](#)
3. Alves Sobrinho, T.; Gómez-Macpherson, H.; Gómez, J.A. A Portable Integrated Rainfall and Overland Flow Simulator. *Soil Use Manag.* **2008**, *24*, 163–170. [\[CrossRef\]](#)
4. Gabrić, O. *Eksperimentalno Istraživanje Procesu Na Slivu: Padavine, Oticaj I Erozijska Tla*; University of Novi Sad: Subotica, Serbia, 2014.
5. Živanović, N.; Rončević, V.; Spasić, M.; Ćorluka, S.; Polovina, S. Construction and Calibration of a Portable Rain Simulator Designed for the in Situ Research of Soil Resistance to Erosion. *Soil Water Res.* **2022**, *17*, 158–169. [\[CrossRef\]](#)
6. Te Chow, V.; Harbaugh, T.E. Raindrop Production for Laboratory Watershed Experimentation. *J. Geophys. Res.* **1965**, *70*, 6111–6119. [\[CrossRef\]](#)
7. Meeuwig, R.O. Infiltration and Water Repellency in Granitic Soils. In *Intermountain Forest & Range Experiment Station*; US Department of Agriculture, Forest Service: Ogden, UT, USA, 1971; volume 111.
8. Battany, M.C.; Grismer, M.E. Development of a Portable Field Rainfall Simulator for Use in Hillside Vineyard Runoff and Erosion Studies. *Hydrol. Process.* **2000**, *14*, 1119–1129. [\[CrossRef\]](#)
9. Naves, J.; Anta, J.; Suárez, J.; Puertas, J. Hydraulic, Wash-off and Sediment Transport Experiments in a Full-Scale Urban Drainage Physical Model. *Sci. Data* **2020**, *7*, 44. [\[CrossRef\]](#)
10. De Ploey, J.; Moeyersons, J. Runoff Creep of Coarse Debris: Experimental Data and Some Field Observations. *Catena* **1975**, *2*, 275–288. [\[CrossRef\]](#)
11. Imeson, A.C. A Simple Field-Portable Rainfall Simulator for Difficult Terrain. *Earth Surf. Process.* **1977**, *2*, 431–436. [\[CrossRef\]](#)
12. Bowyer-Bower, T.A.S.; Burt, T.P. Rainfall Simulators for Investigating Soil Response to Rainfall. *Soil Technol.* **1989**, *2*, 1–16. [\[CrossRef\]](#)
13. Wan, Y.; El-Swaify, S.A. Characterizing Interrill Sediment Size by Partitioning Splash and Wash Processes. *Soil Sci. Soc. Am. J.* **1998**, *62*, 430–437. [\[CrossRef\]](#)
14. Watanabe, H.; Grismer, M.E. Diazinon Transport through Inter-Row Vegetative Filter Strips: Micro-Ecosystem Modeling. *J. Hydrol.* **2001**, *247*, 183–199. [\[CrossRef\]](#)
15. Böker, J.; Zanzinger, H.; Bastian, M.; Németh, E.; Eppel, J. Surface Erosion Control Investigations for a Test Field on a Steep Embankment of German Autobahn A3. In Proceedings of the EuroGeo5, Valencia, Spain, 16–19 September 2012.
16. Flanagan, D.C.; Foster, G.R.; Moldenhauer, W.C. Storm pattern effect on infiltration, runoff, and erosion. *Trans. ASAE* **1988**, *31*, 414–420. [\[CrossRef\]](#)
17. Römken, M.J.; Helming, K.; Prasad, S.N. Soil erosion under different rainfall intensities, surface roughness, and soil water regimes. *Catena* **2002**, *46*, 103–123. [\[CrossRef\]](#)
18. Ran, Q.; Su, D.; Li, P.; He, Z. Experimental Study of the Impact of Rainfall Characteristics on Runoff Generation and Soil Erosion. *J. Hydrol.* **2012**, *424–425*, 99–111. [\[CrossRef\]](#)
19. Mohamadi, M.A.; Kaviani, A. Effects of rainfall patterns on runoff and soil erosion in field plots. *Int. Soil Water Conserv. Res.* **2015**, *3*, 273–281. [\[CrossRef\]](#)

20. Caracciolo, C.; Napoli, M.; Porcù, F.; Prodi, F.; Dietrich, S.; Zanchi, C.; Orlandini, S. Raindrop size distribution and soil erosion. *J. Irrig. Drain. Eng.* **2012**, *138*, 461–469. [\[CrossRef\]](#)
21. Carollo, F.G.; Ferro, V.; Serio, M.A. Estimating Rainfall Erosivity by Aggregated Drop Size Distributions. *Hydrol. Process.* **2016**, *30*, 2119–2128. [\[CrossRef\]](#)
22. Yakubu, M.L.; Yusop, Z.; Fulazzaky, M.A. The Influence of Rain Intensity on Raindrop Diameter and the Kinetics of Tropical Rainfall: Case Study of Skudai, Malaysia. *Hydrol. Sci. J.* **2016**, *61*, 944–951. [\[CrossRef\]](#)
23. Jevtić, L.J. *Hidrologija Bujičnih Tokova*; Šumarski Fakultet Univerziteta u Beogradu: Belgrade, Serbia, 1978.
24. Bisal, F. The Effect of Raindrop Size and Impact Velocity on Sand-Splash. *Can. J. Soil Sci.* **1960**, *40*, 242–245. [\[CrossRef\]](#)
25. Bubenzer, G.D.; Jones, B.A. Drop Size and Impact Velocity Effects on the Detachment of Soils Under Simulated Rainfall. *Trans. ASAE* **1971**, *14*, 625–628.
26. Helming, K. Wind speed effects on rain erosivity. In Proceedings of the Sustaining the global farm—Selected papers from the 10th International Soil Conservation Organization Meeting, West Lafayette, IN, USA, 24–29 May 1999; pp. 771–776.
27. Erpul, G.; Norton, L.D.; Gabriels, D. The effect of wind on raindrop impact and rainsplash detachment. *Trans. ASAE* **2003**, *46*, 51. [\[CrossRef\]](#)
28. Mineo, C.; Ridolfi, E.; Moccia, B.; Russo, F.; Napolitano, F. Assessment of rainfall kinetic-energy-intensity relationships. *Water* **2019**, *11*, 1994. [\[CrossRef\]](#)
29. Sanchez-Moreno, J.F.; Mannaerts, C.M.; Jetten, V.; Löffler-Mang, M. Rainfall kinetic energy-intensity and rainfall momentum-intensity relationships for Cape Verde. *J. Hydrol.* **2012**, *454–455*, 131–140. [\[CrossRef\]](#)
30. Akinola, A.I.; Wynn-Thompson, T.; Olgun, C.G.; Mostaghimi, S.; Eick, M.J. Fluvial erosion rate of cohesive streambanks is directly related to the difference in soil and water temperatures. *J. Environ. Qual.* **2019**, *48*, 1741–1748. [\[CrossRef\]](#)
31. Forti, M.C.; Melfi, A.J.; Astolfo, R.; Fostier, A.H. Rainfall chemistry composition in two ecosystems in the northeastern Brazilian Amazon (Amapá State). *J. Geophys. Res. Atmos.* **2000**, *105*, 28895–28905. [\[CrossRef\]](#)
32. Rončević, V.; Živanović, N.; Ristić, R.; van Boxel, J.H.; Kašanin-Grubin, M. Dripping Rainfall Simulators for Soil Research—Design Review. *Water* **2022**, *14*, 3309. [\[CrossRef\]](#)
33. Ries, J.B.; Iserloh, T. Rainfall Simulation: Methods, Research Questions and Challenges. In Proceedings of the EGU General Assembly, Vienna, Austria, 22–27 April 2012; p. 13866.
34. Yakubu, M.L.; Yusop, Z. Adaptability of Rainfall Simulators as a Research Tool on Urban Sealed Surfaces—A Review. *Hydrol. Sci. J.* **2017**, *62*, 996–1012. [\[CrossRef\]](#)
35. Meyer, L.D.; Harmon, W.C. Multiple-Intensity Rainfall Simulator for Erosion Research on Row Sideslopes. *Trans. ASAE* **1979**, *22*, 0100–0103. [\[CrossRef\]](#)
36. Dunkerley, D.L. Intra-Storm Evaporation as a Component of Canopy Interception Loss in Dryland Shrubs: Observations from Fowlers Gap, Australia. *Hydrol. Process.* **2008**, *22*, 1985–1995. [\[CrossRef\]](#)
37. McCalla, T.M. Water-Drop Method of Determining Stability of Soil Structure. *Soil Sci.* **1944**, *58*, 117–122. [\[CrossRef\]](#)
38. Gunn, R.; Kinzer, G.D. The Terminal Velocity of Fall for Water Droplets in Stagnant Air. *J. Meteorol.* **1949**, *6*, 243–248. [\[CrossRef\]](#)
39. Bruce-Okine, E.; Lal, R. Soil Erodibility as Determined by Raindrop Technique. *Soil Sci.* **1975**, *119*, 149–157. [\[CrossRef\]](#)
40. Cousen, S.M.; Farres, P.J. The Role of Moisture Content in the Stability of Soil Aggregates from a Temperate Silty Soil to Raindrop Impact. *Catena* **1984**, *11*, 313–320. [\[CrossRef\]](#)
41. Sharma, P.P.; Gupta, S.C. Sand Detachment by Single Raindrops of Varying Kinetic Energy and Momentum. *Soil Sci. Soc. Am. J.* **1989**, *53*, 1005–1010. [\[CrossRef\]](#)
42. Mouzai, L.; Bouhade, M. Water Drop Erosivity: Effects on Soil Splash. *J. Hydraul. Res.* **2003**, *41*, 61–68. [\[CrossRef\]](#)
43. Meyer, L.D. Simulation of Rainfall for Soil Erosion Research. *Trans. ASAE* **1965**, *8*, 0063–0065. [\[CrossRef\]](#)
44. McQueen, I.S. *Development of a Hand Portable Rainfall-Simulator Infiltrometer*. Geological Survey; United States Department of the Interior: Washington, DC, USA, 1963; Volume 482.
45. Steinhart, R.; Hillel, D. A Portable Low-Intensity Rain Simulator for Field and Laboratory Use. *Soil Sci. Soc. Am. J.* **1966**, *30*, 661–663. [\[CrossRef\]](#)
46. Hall, M.J. A Critique of Methods of Simulating Rainfall. *Water Resour. Res.* **1970**, *6*, 1104–1114. [\[CrossRef\]](#)
47. Onstad, C.A.; Radke, J.K.; Young, R.A. Outdoor Portable Rainfall Erosion Laboratory. In *Erosion and Sediment Transport Measurement: Symposium IAHS Publication*; International Association of Hydrological Sciences: Wallingford, UK, 1981; Volume 133.
48. Moore, I.D.; Hirschi, M.C.; Barfield, B.J. Kentucky Rainfall Simulator. *Trans. ASAE* **1983**, *26*, 1085–1089. [\[CrossRef\]](#)
49. Joel, A.; Messing, I. Infiltration Rate and Hydraulic Conductivity Measured with Rainfall simulator and Disc Permeameter on Sloping Arid Land. *Arid. Land Res. Manage.* **2001**, *15*, 371–384. [\[CrossRef\]](#)
50. Clarke, M.A.; Walsh, R.P.D. A Portable Rainfall Simulator for Field Assessment of Splash and Slopewash in Remote Locations. *Earth Surf. Process.* **2007**, *32*, 2052–2069. [\[CrossRef\]](#)
51. Parr, J.F.; Bertrand, A.R. Water Infiltration into Soils. *Adv. Agron.* **1960**, *12*, 311–363.
52. Mutchler, C.K.; Hermsmeier, L.F. A Review of Rainfall Simulators. *Trans. ASAE* **1965**, *8*, 0067–0068. [\[CrossRef\]](#)
53. Amerman, C.R. *Proceedings of the Rainfall Simulator Workshop*. Agricultural Research (Western Region); Science and Education Administration, U.S. Department of Agriculture: Oakland, CA, USA, 1979; Volume 10, p. 94612.

54. Cerdá, A. Rainfall Drop Size Distribution in the Western Mediterranean Basin, València, Spain. *CATENA* **1997**, *30*, 169–182. [\[CrossRef\]](#)
55. Ngasoh, F.G.; Mbajjorgu, C.C.; Kamai, M.B.; Okoro, G.O. A Revisit of Rainfall Simulator as a Potential Tool for Hydrological Research. In *Agrometeorology*; IntechOpen: London, UK, 2020.
56. Iserloh, T.; Ries, J.B.; Arnáez, J.; Boix-Fayos, C.; Butzen, V.; Cerdà, A.; Echeverría, M.T.; Fernández-Gálvez, J.; Fister, W.; Geißler, C.; et al. European Small Portable Rainfall Simulators: A Comparison of Rainfall Characteristics. *CATENA* **2013**, *110*, 100–112. [\[CrossRef\]](#)
57. Van Boxel, J.H. Numerical Model for the Fall Speed of Rain Drops in a Rain Fall Simulator. In Proceedings of the Workshop on Wind and Water Erosion, Ghent, Belgium, 17–18 November 1997; pp. 77–85.
58. Malekuti, A.; Gifford, G.F. Natural Vegetation as a Source of Diffuse Salt within the Colorado River Basin. *J. Am. Water Resour. Assoc.* **1978**, *14*, 195–205. [\[CrossRef\]](#)
59. Kamphorst, A. A Small Rainfall Simulator for the Determination of Soil Erodibility. *Neth. J. Agric. Sci.* **1987**, *35*, 407–415. [\[CrossRef\]](#)
60. Harden, C.P.; Mathews, L. Rainfall Response of Degraded Soil Following Reforestation in the Copper Basin, Tennessee, USA. *Environ. Manag.* **2000**, *26*, 163–174. [\[CrossRef\]](#)
61. Iserloh, T.; Pegoraro, D.; Schlösser, A.; Thesing, H.; Seeger, M.; Ries, J.B. Rainfall Simulation Experiments: Influence of Water Temperature, Water Quality and Plot Design on Soil Erosion and Runoff. In Proceedings of the EGU General Assembly, Vienna, Austria, 12–17 April 2015.
62. Green, T.; Houk, D.F. The Mixing of Rain with Near-Surface Water. *J. Fluid Mech.* **1979**, *90*, 569. [\[CrossRef\]](#)
63. Agassi, M.; Bloem, D.; Ben-Hur, M. Effect of Drop Energy and Soil and Water Chemistry on Infiltration and Erosion. *Water Resour. Res.* **1994**, *30*, 1187–1193. [\[CrossRef\]](#)
64. Xiao, H.; Liu, G.; Abd-Elbasit, M.A.M.; Zhang, X.C.; Liu, P.L.; Zheng, F.L.; Zhang, J.Q.; Hu, F.N. Effects of Slaking and Mechanical Breakdown on Disaggregation and Splash Erosion: Effects of Splash Erosion on Aggregate Breakdown. *Eur. J. Soil Sci.* **2017**, *68*, 797–805. [\[CrossRef\]](#)
65. Rončević, V.; Živanović, N.; Boxel, J.H.V.; Iserloh, T.; Antić, N. Measuring the Size of Pendant Water Drop Generated by Hypodermic Needles for Construction of Rainfall Simulator for Soil Research. *Water* **2023**. *manuscript in preparation*.
66. Boucher, E.A.; Evans, M.J.B. Pendant Drop Profiles and Related Capillary Phenomena. *Proc. R. Soc. London. A. Math. Phys. Sci.* **1975**, *346*, 349–374. [\[CrossRef\]](#)
67. Mutchler, C.K.; Moldenhauer, W.C. Applicator for Laboratory Rainfall Simulator. *Trans. ASAE* **1963**, *6*, 0220–0222. [\[CrossRef\]](#)
68. Harkins, W.D.; Brown, F.E. The Determination of Surface Tension (Free Surface Energy), and the Weight of Falling Drops: The Surface Tension of Water and Benzene by the Capillary Height Method. *J. Am. Chem. Soc.* **1919**, *41*, 499–524. [\[CrossRef\]](#)
69. Henderson, D.C.; Micale, F.J. Dynamic Surface Tension Measurement with the Drop Mass Technique. *J. Colloid Interface Sci.* **1993**, *158*, 289–294. [\[CrossRef\]](#)
70. Xu, Y. Dynamic Interfacial Tension between Bitumen and Aqueous Sodium Hydroxide Solutions. *Energy Fuels* **1995**, *9*, 148–154. [\[CrossRef\]](#)
71. Pu, B.; Chen, D. A Study of the Measurement of Surface and Interfacial Tension by the Maximum Liquid Drop Volume Method. *J. Colloid Interface Sci.* **2001**, *235*, 265–272. [\[CrossRef\]](#)
72. Lee, B.-B.; Ravindra, P.; Chan, E.-S. A Critical Review: Surface and Interfacial Tension Measurement by the Drop Weight Method. *Chem. Eng. Commun.* **2008**, *195*, 889–924. [\[CrossRef\]](#)
73. Hozawa, M.; Tsukada, T.; Imaishi, N.; Fujinwa, K. Effect of Wettability on Static Drop Formation from a Hole in Horizontal Flat Plate. *J. Chem. Eng. Jpn.* **1981**, *14*, 358–364. [\[CrossRef\]](#)
74. Miller, R.; Schano, K.-H.; Hofmann, A. Hydrodynamic Effects in Measurements with the Drop Volume Technique at Small Drop Times 1. Surface Tensions of Pure Liquids and Mixtures. *Colloids Surf. A: Physicochem. Eng. Asp.* **1994**, *92*, 189–196. [\[CrossRef\]](#)
75. Garandet, J.P.; Vinet, B.; Gros, P. Considerations on the Pendant Drop Method: A New Look at Tate's Law and Harkins' Correction Factor. *J. Colloid Interface Sci.* **1994**, *165*, 351–354. [\[CrossRef\]](#)
76. Portuguese, E.; Alzina, A.; Michaud, P.; Oudjedi, M.; Smith, A. Evolution of a Water Pendant Droplet: Effect of Temperature and Relative Humidity. *Nat. Sci.* **2017**, *9*, 1–20. [\[CrossRef\]](#)
77. Barry, P.V.; Turco, R.F.; Stott, D.E.; Bradford, J.M. Organic Polymers' Effect on Soil Shear Strength and Detachment by Single Raindrops. *Soil Sci. Soc. Am. J.* **1991**, *55*, 799–804. [\[CrossRef\]](#)
78. Bissonnais, Y.L.; Singer, M.J. Crusting, Runoff, and Erosion Response to Soil Water Content and Successive Rainfalls. *Soil Sci. Soc. Am. J.* **1992**, *56*, 1898–1903. [\[CrossRef\]](#)
79. Black, P.E. Runoff from Watershed Models. *Water Resour. Res.* **1970**, *6*, 465–477. [\[CrossRef\]](#)
80. Houk, D.; Green, T. A Note on Surface Waves Due to Rain. *J. Geophys. Res.* **1976**, *81*, 4482–4484. [\[CrossRef\]](#)
81. Moss, A.J.; Green, T.W. Erosive Effects of the Large Water Drops (Gravity Drops) That Fall from Plants. *Soil Res.* **1987**, *25*, 9. [\[CrossRef\]](#)
82. Robinson, D.A.; Naghizadeh, R. The Impact of Cultivation Practice and Wheelings on Runoff Generation and Soil Erosion on the South Downs: Some Experimental Results Using Simulated Rainfall. *Soil Use Manag.* **1992**, *8*, 151–156. [\[CrossRef\]](#)
83. Ao, C.; Yang, P.; Zeng, W.; Chen, W.; Xu, Y.; Xu, H.; Zha, Y.; Wu, J.; Huang, J. Impact of Raindrop Diameter and Polyacrylamide Application on Runoff, Soil and Nitrogen Loss via Raindrop Splashing. *Geoderma* **2019**, *353*, 372–381. [\[CrossRef\]](#)

84. Wang, L.; Fang, N.F.; Yue, Z.J.; Shi, Z.H.; Hua, L. Raindrop Size and Flow Depth Control Sediment Sorting in Shallow Flows on Steep Slopes. *Water Resour. Res.* **2018**, *54*, 9978–9995. [\[CrossRef\]](#)
85. Walker, P.H.; Hutka, J.; Moss, A.J.; Kinnell, P.I.A. Use of a Versatile Experimental System for Soil Erosion Studies. *Soil Sci. Soc. Am. J.* **1977**, *41*, 610–612. [\[CrossRef\]](#)
86. Riezebos, H.T.; Epema, G.F. Drop Shape and Erosivity Part II: Splash Detachment, Transport and Erosivity Indices. *Earth Surf. Process.* **1985**, *10*, 69–74. [\[CrossRef\]](#)
87. Moss, A.J. Effects of Flow Velocity Variation on Rain Driven Transportation and the Role of Rain Impact in the Movement of Solids. *Soil Res.* **1988**, *26*, 443. [\[CrossRef\]](#)
88. Chevone, B.I.; Yang, Y.S.; Winner, W.E.; Storks-Cotter, I.; Long, S.J. A Rainfall Simulator for Laboratory Use in Acidic Precipitation Studies. *J. Air Pollut. Control Assoc.* **1984**, *34*, 355–359. [\[CrossRef\]](#)
89. Abu-Zreig, M. Control of Rainfall-Induced Soil Erosion with Various Types of Polyacrylamide (8 pp). *J. Soils Sediments* **2006**, *6*, 137–144. [\[CrossRef\]](#)
90. Magarvey, R.H.; Taylor, B.W. Apparatus for the Production of Large Water Drops. *Rev. Sci. Instrum.* **1956**, *27*, 944–947. [\[CrossRef\]](#)
91. Brakensiek, D.L.; Rawls, W.J.; Hamon, W.R. Application of an Infiltrometer System for Describing Infiltration into Soils. *Trans. ASAE* **1979**, *22*, 320–325. [\[CrossRef\]](#)
92. Bhardwaj, A.; Singh, R. Development of a Portable Rainfall Simulator Infiltrometer for Infiltration, Runoff and Erosion Studies. *Agric. Water Manag.* **1992**, *22*, 235–248. [\[CrossRef\]](#)
93. Thompson, A.L.; Ghidry, F.; Regmi, T.P. Raindrop Energy Effects on Chemical and Sediment Transport. *Trans. ASAE* **2001**, *44*, 835. [\[CrossRef\]](#)
94. Cerdà, A.; Ibáñez, S.; Calvo, A. Design and Operation of a Small and Portable Rainfall Simulator for Rugged Terrain. *Soil Technol.* **1997**, *11*, 163–170. [\[CrossRef\]](#)
95. Ristić, R.; Malošević, D. *Hidrologija Bujičnih Tokova*; Univerzitet u Beogradu, Šumarski Fakultet: Belgrade Serbia, 2011.
96. Pruppacher, H.R.; Klett, J.D. Microphysics of Clouds and Precipitation. *Nature* **2012**, *284*, 88. [\[CrossRef\]](#)
97. Blanchard, D.C. The Behavior of Water Drops at Terminal Velocity in Air. *Trans. Am. Geophys. Union* **1950**, *31*, 836. [\[CrossRef\]](#)
98. Hudson, N.W. *Soil Conservation*; Scientific Publishers: New Delhi, India, 2015.
99. Brandt, C.J. The Size Distribution of Throughfall Drops under Vegetation Canopies. *CATENA* **1989**, *16*, 507–524. [\[CrossRef\]](#)
100. Coutinho, M.A.; Tomás, P.P. Characterization of Raindrop Size Distributions at the Vale Formoso Experimental Erosion Center. *CATENA* **1995**, *25*, 187–197. [\[CrossRef\]](#)
101. Nyssen, J.; Vandenreyken, H.; Poesen, J.; Moeyersons, J.; Deckers, J.; Haile, M.; Salles, C.; Govers, G. Rainfall Erosivity and Variability in the Northern Ethiopian Highlands. *J. Hydrol.* **2005**, *311*, 172–187. [\[CrossRef\]](#)
102. Meshesha, D.T.; Tsunekawa, A.; Haregeweyn, N. Influence of Raindrop Size on Rainfall Intensity, Kinetic Energy, and Erosivity in a Sub-Humid Tropical Area: A Case Study in the Northern Highlands of Ethiopia. *Theor. Appl. Climatol.* **2019**, *136*, 1221–1231. [\[CrossRef\]](#)
103. Carter, C.E.; Greer, J.D.; Braud, H.J.; Floyd, J.M. Raindrop Characteristics in South Central United States. *Trans. ASAE* **1974**, *17*, 1033–1037. [\[CrossRef\]](#)
104. Laws, J.O. Measurements of the Fall-Velocity of Water -Drops and Raindrops. *Trans. Am. Geophys. Union* **1941**, *22*, 709. [\[CrossRef\]](#)
105. Reichard, D.L. A System for Producing Various Sizes, Numbers, and Frequencies of Uniform-Size Drops. *Trans. ASAE* **1990**, *33*, 1767–1770. [\[CrossRef\]](#)
106. Macklin, W.C.; Hobbs, P.V. Subsurface Phenomena and the Splashing of Drops on Shallow Liquids. *Science* **1969**, *166*, 107–108. [\[CrossRef\]](#) [\[PubMed\]](#)
107. Rose, C.W. Soil Detachment Caused by Rainfall. *Soil Sci.* **1960**, *89*, 28–35. [\[CrossRef\]](#)
108. Roth, C.H.; Meyer, B.; Frede, H.-G. A Portable Rainfall Simulator for Studying Factors Affecting Runoff, Infiltration and Soil Loss. *Catena* **1985**, *12*, 79–85. [\[CrossRef\]](#)
109. Thompson, A.L.; James, L.G. Water Droplet Impact and Its Effect on Infiltration. *Trans. ASAE* **1985**, *28*, 1506–1510. [\[CrossRef\]](#)
110. Regmi, T.P.; Thompson, A.L. Rainfall Simulator for Laboratory Studies. *Appl. Eng. Agric.* **2000**, *16*, 641–647. [\[CrossRef\]](#)
111. Brandt, C.J. Simulation of the Size Distribution and Erosivity of Raindrops and Throughfall Drops. *Earth Surf. Process. Landf.* **1990**, *15*, 687–698. [\[CrossRef\]](#)
112. Carollo, F.G.; Ferro, V.; Serio, M.A. Predicting Rainfall Erosivity by Momentum and Kinetic Energy in Mediterranean Environment. *J. Hydrol.* **2018**, *560*, 173–183. [\[CrossRef\]](#)
113. Laws, J.O.; Parsons, D.A. The Relation of Raindrop-Size to Intensity. *Trans. Am. Geophys. Union* **1943**, *24*, 452. [\[CrossRef\]](#)
114. Atlas, D. OPTICAL EXTINCTION by RAINFALL. *J. Meteorol.* **1953**, *10*, 486–488. [\[CrossRef\]](#)
115. Zanchi, C.; Torri, D. *Evaluation of Rainfall Energy in Central Italy. Assessment of Erosion*; John Wiley and Sons Ltd.: Hoboken, NJ, USA, 1980; pp. 133–142.
116. Jayawardena, A.W.; Rezaur, R.B. Drop Size Distribution and Kinetic Energy Load of Rainstorms in Hong Kong. *Hydrol. Process.* **2000**, *14*, 1069–1082. [\[CrossRef\]](#)
117. Kinnell, P.I.A. Rainfall Intensity-Kinetic Energy Relationships for Soil Loss Prediction1. *Soil Sci. Soc. Am. J.* **1981**, *45*, 153. [\[CrossRef\]](#)
118. Rosewell, C.J. Rainfall Kinetic Energy in Eastern Australia. *J. Clim. Appl. Meteorol.* **1986**, *25*, 1695–1701. [\[CrossRef\]](#)
119. Brown, L.C.; Foster, G.R. Storm Erosivity Using Idealized Intensity Distributions. *Trans. ASAE* **1987**, *30*, 0379–0386. [\[CrossRef\]](#)

120. Carollo, F.G.; Ferro, V.; Serio, M.A. Reliability of Rainfall Kinetic Power-Intensity Relationships. *Hydrol. Process.* **2017**, *31*, 1293–1300. [\[CrossRef\]](#)
121. Hudson, N.W. *The Influence of Rainfall on the Mechanics of Soil Erosion: With Particular Reference to Southern Rhodesia*; University of Cape Town: Cape Town, South Africa, 1965.
122. Assouline, S.; Mualem, Y. The Similarity of Regional Rainfall: A Dimensionless Model of Drop Size Distribution. *Trans. ASAE* **1989**, *32*, 1216–1222. [\[CrossRef\]](#)
123. Van Dijk, A.I.J.M.; Bruijnzeel, L.A.; Rosewell, C.J. Rainfall Intensity-Kinetic Energy Relationships: A Critical Literature Appraisal. *J. Hydrol.* **2002**, *261*, 1–23. [\[CrossRef\]](#)
124. Mueller, E.A.; Sims, A.L. *Raindrop Distributions at Island Beach, New Jersey*; Atmospheric Sciences Laboratory, US Army Electronics Command: Fort Monmouth, NJ, USA, 1967.
125. Mueller, E.A.; Sims, A.L. *Raindrop Distributions at Corvallis, Oregon*; US Army Electronics Command: Fort Monmouth, NJ, USA, 1968.
126. Mason, B.J.; Andrews, J.B. Drop-Size Distributions from Various Types of Rain. *Q. J. R. Meteorol. Soc.* **1960**, *86*, 346–353. [\[CrossRef\]](#)
127. Sauvageot, H.; Lacaux, J.-P. The Shape of Averaged Drop Size Distributions. *J. Atmos. Sci.* **1995**, *52*, 1070–1083. [\[CrossRef\]](#)
128. McCool, D.K.; Williams, J.D.; Morse, J.R. Raindrop Characteristics in the Pacific Northwest. In Proceedings of the ASABE Annual International Meeting, Reno, NV, USA, 21–24 June 2009.
129. Llasat, M.-C. An Objective Classification of Rainfall Events on the Basis of Their Convective Features: Application to Rainfall Intensity in the Northeast of Spain. *Int. J. Climatol.* **2001**, *21*, 1385–1400. [\[CrossRef\]](#)
130. Hadadin, A.N. Rainfall Intensity-Duration-Frequency Relationship in the Mujib Basin in Jordan. *J. Appl. Sci.* **2005**, *5*, 1777–1784. [\[CrossRef\]](#)
131. AlHassoun, S.A. Developing an Empirical Formulae to Estimate Rainfall Intensity in Riyadh Region. *J. King Saud Univ.-Eng. Sci.* **2011**, *23*, 81–88. [\[CrossRef\]](#)
132. Ologhadien, I.; Nwaogazie, I.L. Rainfall Intensity-Duration-Frequency Models for Selected Cities in Southern Nigeria. *Stand. Sci. Res. Essays* **2014**, *2*, 509–515.
133. Lubrica, N.V.; Villanueva, J.R.; Daligdig, J.; Telino, G.; Puyongan, M.D.; Jimenez, V.; Aguilar, A.; delos Reyes, W. Revisiting the Adequacy of the Existing Drainage System Using the Rational Method and Geographic Information System. *Tangkoyob UC Res. J.* **2015**, *9*, 5–17.
134. Best, A.C. The Size Distribution of Raindrops. *Q. J. R. Meteorol. Soc.* **1950**, *76*, 16–36. [\[CrossRef\]](#)
135. Beard, K.V.; Pruppacher, H.R. A Determination of the Terminal Velocity and Drag of Small Water Drops by Means of a Wind Tunnel. *J. Atmos. Sci.* **1969**, *26*, 1066–1072. [\[CrossRef\]](#)
136. Uplinger, W.G. A New Formula for Raindrop Terminal Velocity. In Proceedings of the 20th Conference on Radar Meteorology, Boston, MA, USA, 30 November–3 December 1981; pp. 389–391.
137. Adams, J.E.; Kirkham, D.; Nielsen, D.R. A Portable Rainfall-Simulator Infiltrometer and Physical Measurements of Soil in Place. *Soil Sci. Soc. Am. J.* **1957**, *21*, 473–477. [\[CrossRef\]](#)
138. Ahuja, L.R. Modeling Soluble Chemical Transfer to Runoff with Rainfall Impact as a Diffusion Process. *Soil Sci. Soc. Am. J.* **1990**, *54*, 312–321. [\[CrossRef\]](#)
139. Ahuja, L.R.; Lehman, O.R. The Extent and Nature of Rainfall—Soil Interaction in the Release of Soluble Chemicals to Runoff. *J. Environ. Qual.* **1983**, *12*, 34–40. [\[CrossRef\]](#)
140. Ahuja, L.R.; Lehman, O.R.; Sharpley, A.N. Bromide and Phosphate in Runoff Water from Shaped and Cloddy Soil Surfaces. *Soil Sci. Soc. Am. J.* **1983**, *47*, 746–748. [\[CrossRef\]](#)
141. Andersen, C.T.; Foster, I.D.L.; Pratt, C.J. The Role of Urban Surfaces (Permeable Pavements) in Regulating Drainage and Evaporation: Development of a Laboratory Simulation Experiment. *Hydrol. Process.* **1999**, *13*, 597–609. [\[CrossRef\]](#)
142. Aston, A.R. Rainfall Interception by Eight Small Trees. *J. Hydrol.* **1979**, *42*, 383–396. [\[CrossRef\]](#)
143. Barnes, O.K.; Costel, G. A Mobile Infiltrometer 1. *Agron. J.* **1957**, *49*, 105–107. [\[CrossRef\]](#)
144. Blackburn, W.H. Simulated Rainfall Studies of Selected Plant Communities and Soils in Five Rangeland Watersheds of Nevada. Ph.D. Thesis, University of Nevada, Reno, NV, USA, 1973.
145. Blackburn, W.H.; Meeuwig, R.O.; Skau, C.M. A Mobile Infiltrometer for Use on Rangeland. *J. Range Manag.* **1974**, *27*, 322. [\[CrossRef\]](#)
146. Boers, T.M.; van Deurzen, F.J.M.P.; Eppink, L.A.A.J.; Ruytenberg, R.E. Comparison of Infiltration Rates Measured with an Infiltrometer, a Rainulator and a Permeameter for Erosion Research in SE Nigeria. *Soil Technol.* **1992**, *5*, 13–26. [\[CrossRef\]](#)
147. Carrà, B.G.; Bombino, G.; Denisi, P.; Plaza-Álvarez, P.A.; Lucas-Borja, M.E.; Zema, D.A. Water Infiltration after Prescribed Fire and Soil Mulching with Fern in Mediterranean Forests. *Hydrology* **2021**, *8*, 95. [\[CrossRef\]](#)
148. Cerdà, A.; García-Fayos, P. The Influence of Seed Size and Shape on Their Removal by Water Erosion. *Catena* **2002**, *48*, 293–301. [\[CrossRef\]](#)
149. Commandeur, P.R. Soil Erosion Studies Using Rainfall Simulation on Forest Harvested Areas in British Columbia. In Proceedings of the International Symposium on Erosion, Debris Flows and Environment in Mountain Regions, Chengdu, China, 5–9 July 1992; IAHS Publication: Oxfordshire, UK, 1992; pp. 21–23.
150. Corona, R.; Wilson, T.; D’Adderio, L.P.; Porcù, F.; Montaldo, N.; Albertson, J. On the Estimation of Surface Runoff through a New Plot Scale Rainfall Simulator in Sardinia, Italy. *Procedia Environ. Sci.* **2013**, *19*, 875–884. [\[CrossRef\]](#)

151. Danacova, M. The Impact of Slope Gradients on the Generation of Surface Runoff in Laboratory Conditions. In Proceedings of the 17th International Multidisciplinary Scientific GeoConference SGEM2017, Water Resources, Forest, Marine and Ocean Ecosystems, Vienna, Austria, 27–29 November 2017.
152. Dalgleish, H.Y.; Foster, I.D.L. 137Cs Losses from a Loamy Surface Water Gleyed Soil (Inceptisol); a Laboratory Simulation Experiment. *Catena* **1996**, *26*, 227–245. [\[CrossRef\]](#)
153. De Ploey, J. A Stemflow Equation for Grasses and Similar Vegetation. *Catena* **1982**, *9*, 139–152. [\[CrossRef\]](#)
154. De Ploey, J.; Múcher, H.J. A Consistency Index and Rainwash Mechanisms on Belgian Loamy Soils. *Earth Surf. Process.* **1981**, *6*, 319–330. [\[CrossRef\]](#)
155. Dimoyiannis, D.G.; Valmis, S.; Vyrlas, P. A Rainfall Simulation Study of Erosion of Some Calcareous Soils. *Glob. Nest* **2001**, *3*, 179–183.
156. Dunkerley, D. Effects of Rainfall Intensity Fluctuations on Infiltration and Runoff: Rainfall Simulation on Dryland Soils, Fowlers Gap, Australia: Rainfall Intensity Fluctuations in Fowlers Gap. *Hydrol. Process.* **2012**, *26*, 2211–2224. [\[CrossRef\]](#)
157. Ekern, P.C., Jr.; Muckenhirn, R.J. Water Drop Impact as a Force in Transporting Sand. *Soil Sci. Soc. Am. J.* **1948**, *12*, 441–444. [\[CrossRef\]](#)
158. Ellison, W.D.; Pomerene, W.H. A Rainfall Applicator. *Agric. Eng.* **1944**, *25*, 220.
159. Epstein, E.; Grant, W.J. TB22: Design, Construction and Calibration of a Laboratory Rainfall Simulator. Technical Bulletins of the Maine Agricultural & Forest Experiment Station. 1966. Available online: <https://core.ac.uk/download/pdf/217132135.pdf> (accessed on 17 January 2023).
160. Farres, P.J. The Dynamics of Rainsplash Erosion and the Role of Soil Aggregate Stability. *Catena* **1987**, *14*, 119–130. [\[CrossRef\]](#)
161. Fernández-Gálvez, J.; Barahona, E.; Mingorance, M.D. Measurement of Infiltration in Small Field Plots by a Portable Rainfall Simulator: Application to Trace-Element Mobility. *Water Air Soil Pollut.* **2008**, *191*, 257–264. [\[CrossRef\]](#)
162. Foley, J.L.; Silburn, D.M. Hydraulic Properties of Rain Impact Surface Seals on Three Clay Soils-Influence of Raindrop Impact Frequency and Rainfall Intensity during Steady State. *Soil Res.* **2002**, *40*, 1069–1083. [\[CrossRef\]](#)
163. Foster, I.D.L.; Fullen, M.A.; Brandsma, R.T.; Chapman, A.S. Drip-Screen Rainfall Simulators for Hydro- and Pedo-Geomorphological Research: The Coventry Experience. *Earth Surf. Process. Landf.* **2000**, *25*, 691–707. [\[CrossRef\]](#)
164. Freebairn, D.M.; Gupta, S.C. Microrelief, Rainfall and Cover Effects on Infiltration. *Soil Tillage Res.* **1990**, *16*, 307–327. [\[CrossRef\]](#)
165. Fu, Y.; Li, G.-L.; Zheng, T.-H.; Li, B.-Q.; Zhang, T. Splash Detachment and Transport of Loess Aggregate Fragments by Raindrop Action. *Catena* **2017**, *150*, 154–160. [\[CrossRef\]](#)
166. Gabriels, D.; De Boodt, M. Erosion Reduction Factors for Chemically Treated Soils: A Laboratory Experiment. In *SSSA Special Publications*; Soil Science Society of America: Madison, WI, USA, 1975; pp. 95–102.
167. Gabriels, D.; Moldenhauer, W.C. Size Distribution of Eroded Material from Simulated Rainfall: Effect over a Range of Texture. *Soil Sci. Soc. Am. J.* **1978**, *42*, 954–958. [\[CrossRef\]](#)
168. Gao, B.; Todd Walter, M.; Steenhuis, T.S.; Hogarth, W.L.; Parlange, J.-Y. Rainfall Induced Chemical Transport from Soil to Runoff: Theory and Experiments. *J. Hydrol.* **2004**, *295*, 291–304. [\[CrossRef\]](#)
169. Gao, B.; Walter, M.T.; Steenhuis, T.S.; Parlange, J.-Y.; Nakano, K.; Rose, C.W.; Hogarth, W.L. Investigating Ponding Depth and Soil Detachability for a Mechanistic Erosion Model Using a Simple Experiment. *J. Hydrol.* **2003**, *277*, 116–124. [\[CrossRef\]](#)
170. Gao, B.; Walter, M.T.; Steenhuis, T.S.; Parlange, J.-Y.; Richards, B.K.; Hogarth, W.L.; Rose, C.W. Investigating Raindrop Effects on Transport of Sediment and Non-Sorbed Chemicals from Soil to Surface Runoff. *J. Hydrol.* **2005**, *308*, 313–320. [\[CrossRef\]](#)
171. Goodman, L.J. Erosion Control in Engineering Works. *Agric. Eng.* **1952**, *33*, 155–157.
172. Guerrant, D.G.; Miller, W.W.; Mahannah, C.N.; Narayanan, R. Infiltration Evaluation of Four Mechanical Rainfall Simulation Techniques in Sierra Nevada Watersheds 1. *Jawra J. Am. Water Resour. Assoc.* **1990**, *26*, 127–134. [\[CrossRef\]](#)
173. Guerrant, D.G.; Miller, W.W.; Mahannah, C.N.; Narayanan, R. Site—Specific Erosivity Evaluation of a Sierra Nevada Forested Watershed Soil. *J. Environ. Qual.* **1991**, *20*, 396–402. [\[CrossRef\]](#)
174. Healy, M.G.; Fenton, O.; Cummins, E.; Clarke, R.; Peyton, D.; Fleming, G.; Wall, D.; Morrison, L.; Cormican, M. Health and Water Quality Impacts Arising from Land Spreading of Biosolids. *Environ. Prot. Agency Res. Rep.* **2017**, *200*. [\[CrossRef\]](#)
175. Heathwaite, A.L.; Johnes, P.J. Contribution of Nitrogen Species and Phosphorus Fractions to Stream Water Quality in Agricultural Catchments. *Hydrol. Process.* **1996**, *10*, 971–983. [\[CrossRef\]](#)
176. Heilig, A.; DeBruyn, D.; Walter, M.T.; Rose, C.W.; Parlange, J.-Y.; Steenhuis, T.S.; Sander, G.C.; Hairsine, P.B.; Hogarth, W.L.; Walker, L.P. Testing a Mechanistic Soil Erosion Model with a Simple Experiment. *J. Hydrol.* **2006**, *317*, 171–172. [\[CrossRef\]](#)
177. Herwitz, S.R. Interception Storage Capacities of Tropical Rainforest Canopy Trees. *J. Hydrol.* **1985**, *77*, 237–252. [\[CrossRef\]](#)
178. Hignett, C.T.; Gusli, S.; Cass, A.; Besz, W. An Automated Laboratory Rainfall Simulation System with Controlled Rainfall Intensity, Raindrop Energy and Soil Drainage. *Soil Technol.* **1995**, *8*, 31–42. [\[CrossRef\]](#)
179. Hlavčová, K.; Danáčová, M.; Kohnová, S.; Szolgay, J.; Valent, P.; Výleta, R. Estimating the Effectiveness of Crop Management on Reducing Flood Risk and Sediment Transport on Hilly Agricultural Land—A Myjava Case Study, Slovakia. *Catena* **2019**, *172*, 678–690. [\[CrossRef\]](#)
180. Huang, J.; Wu, P.; Zhao, X. Effects of Rainfall Intensity, Underlying Surface and Slope Gradient on Soil Infiltration under Simulated Rainfall Experiments. *Catena* **2013**, *104*, 93–102. [\[CrossRef\]](#)
181. Jeppson, R.W.; Rawls, W.J.; Hamon, W.R.; Schreiber, D.L. Use of Axisymmetric Infiltration Model and Field Data to Determine Hydraulic Properties of Soils. *Water Resour. Res.* **1975**, *11*, 127–138. [\[CrossRef\]](#)

182. Kinnell, P.I.A. Laboratory Studies on the Effect of Drop Size on Splash Erosion. *J. Agric. Eng. Res.* **1982**, *27*, 431–439. [\[CrossRef\]](#)
183. Kinnell, P.I.A. Particle Travel Distances and Bed and Sediment Compositions Associated with Rain-Impacted Flows. *Earth Surf. Process.* **2001**, *26*, 749–758. [\[CrossRef\]](#)
184. Kinnell, P.I.A. Sediment Transport by Medium to Large Drops Impacting Flows at Subterminal Velocity. *Soil Sci. Soc. Am. J.* **2005**, *69*, 902–905. [\[CrossRef\]](#)
185. Kinnell, P.I.A. Splash Erosion: Some Observations on the Splash-Cup Technique. *Soil Sci. Soc. Am. J.* **1974**, *38*, 657–660. [\[CrossRef\]](#)
186. Kinnell, P.I.A. The Influence of Flow Discharge on Sediment Concentrations in Raindrop Induced Flow Transport. *Soil Res.* **1988**, *26*, 575. [\[CrossRef\]](#)
187. Levin, J.; Ben-Hur, M.; Gal, M.; Levy, G.J. Rain Energy and Soil Amendments Effects on Infiltration and Erosion of Three Different Soil Types. *Soil Res.* **1991**, *29*, 455. [\[CrossRef\]](#)
188. Lu, J.-Y.; Chen, J.-Y.; Chang, F.-H.; Lu, T.-F. Characteristics of Shallow Rain-Impacted Flow over Smooth Bed. *J. Hydraul. Eng.* **1998**, *124*, 1242–1252. [\[CrossRef\]](#)
189. Lu, J.-Y.; Chen, J.-Y.; Hong, J.-H.; Lu, T.-F.; Liu, C.-S. Turbulence Intensities of Shallow Rain-Impacted Flow over Rough Bed. *J. Hydraul. Eng.* **2001**, *127*, 881–886. [\[CrossRef\]](#)
190. Lu, J.-Y.; Lee, J.-J.; Lu, T.-F.; Hong, J.-H. Experimental Study of Extreme Shear Stress for Shallow Flow under Simulated Rainfall. *Hydrol. Process.* **2009**, *23*, 1660–1667. [\[CrossRef\]](#)
191. Moore, J.M.; Mihara, M. Development of Portable Artificial Rainfall Simulator for Evaluating Sustainable Farming in Kenya. *Int. J. Environ. Rural. Dev.* **2017**, *8*, 27–33.
192. McIntyre, D.S. Permeability Measurements of Soil Crusts Formed by Raindrop Impact. *Soil Sci.* **1958**, *85*, 185–189. [\[CrossRef\]](#)
193. McIntyre, D.S. Soil Splash and the Formation of Surface Crusts by Raindrop Impact. *Soil Sci.* **1958**, *85*, 261–266. [\[CrossRef\]](#)
194. Mohanty, S.; Singh, R. Determination of Soil Hydrologic Properties under Simulated Rainfall Condition. *Agric. Water Manag.* **1996**, *29*, 267–281. [\[CrossRef\]](#)
195. Mohr, C.; Anton, H. *Design and Application of a Drip-Type Rainfall Simulator Adapted to Steep Topography and Low Intensity-Rainfall Characteristics in the Coastal Range of Southern Chile*. EGU General Assembly Conference Abstracts. 2010. Available online: <https://meetingorganizer.copernicus.org/EGU2010/EGU2010-7350-1.pdf> (accessed on 17 January 2023).
196. Mohr, C.H.; Coppus, R.; Iroumé, A.; Huber, A.; Bronstert, A. Runoff Generation and Soil Erosion Processes after Clear Cutting: Runoff and Erosion After Clear Cutting. *J. Geophys. Res. Earth Surf.* **2013**, *118*, 814–831. [\[CrossRef\]](#)
197. Moldenhauer, W.C.; Kemper, W.D. Interdependence of Water Drop Energy and Clod Size on Infiltration and Clod Stability. *Soil Sci. Soc. Am. J.* **1969**, *33*, 297–301. [\[CrossRef\]](#)
198. Moldenhauer, W.C.; Koswara, J. Effect of Initial Clod Size on Characteristics of Splash and Wash Erosion1. *Soil Sci. Soc. Am. J.* **1968**, *32*, 875. [\[CrossRef\]](#)
199. Moldenhauer, W.C.; Long, D.C. Influence of Rainfall Energy on Soil Loss and Infiltration Rates: I. Effect over a Range of Texture. *Soil Sci. Soc. Am. J.* **1964**, *28*, 813–817. [\[CrossRef\]](#)
200. Moore, D.C.; Singer, M.J. Crust Formation Effects on Soil Erosion Processes. *Soil Sci. Soc. Am. J.* **1990**, *54*, 1117–1123. [\[CrossRef\]](#)
201. Moss, A.J.; Green, P. Movement of Solids in Air and Water by Raindrop Impact. Effects of Drop-Size and Water-Depth Variations. *Soil Res.* **1983**, *21*, 257. [\[CrossRef\]](#)
202. Moss, A.J.; Walker, P.H.; Hutka, J. Raindrop-Stimulated Transportation in Shallow Water Flows: An Experimental Study. *Sediment. Geol.* **1979**, *22*, 165–184. [\[CrossRef\]](#)
203. Munn, J.R.; Huntington, G.L. A Portable Rainfall Simulator for Erodibility and Infiltration Measurements on Rugged Terrain. *Soil Sci. Soc. Am. J.* **1976**, *40*, 622–624. [\[CrossRef\]](#)
204. Nampulá, J.L.C.; Lara, C.M.G.; Medinilla, E.E.; Herrera, R.G.; Toledo, P.V.; Sánchez, R.A.V. Diseño y Calibración de Un Simulador Automático de Lluvia. *Espac. I+D Innovación Más Desarro.* **2016**, *5*, 23–37. [\[CrossRef\]](#)
205. Naslas, G.D.; Miller, W.W.; Gifford, G.F.; Fernandez, G.C.J. Effects of Soil Type, Plot Condition, and Slope on Runoff and Interrill Erosion of Two Soils in the Lake Tahoe Basin 1. *Jawra J. Am. Water Resour. Assoc.* **1994**, *30*, 319–328. [\[CrossRef\]](#)
206. Naves, J.; Anta, J.; Suárez, J.; Puertas, J. Development and Calibration of a New Dripper-Based Rainfall Simulator for Large-Scale Sediment Wash-off Studies. *Water* **2020**, *12*, 152. [\[CrossRef\]](#)
207. Norton, L.D. Micromorphological Study of Surface Seals Developed under Simulated Rainfall. *Geoderma* **1987**, *40*, 127–140. [\[CrossRef\]](#)
208. Osborn, B. *Measuring Soil Splash and Protective Value of Cover on Range Land: Methods and Equipment Used in Range Cover Evaluations in Texas and Oklahoma*; US Department of Agriculture, Soil Conservation Service: Washington, DC, USA, 1949.
209. Parlak, M. Determination of Soil Erosion over Different L and Uses by Mini Rainfall Simulator. *J. Food Agric. Environ.* **2012**, *10*, 929–933.
210. Rasbash, D.J. The Production of Water Spray of Uniform Drop Size by a Battery of Hypodermic Needles. *J. Sci. Instrum.* **1953**, *30*, 189–192. [\[CrossRef\]](#)
211. Riezebos, T.H.; Seyhan, E. Essential Conditions of Rainfall Simulation for Laboratory Water Erosion Experiments. *Earth Surf. Process.* **1977**, *2*, 185–190. [\[CrossRef\]](#)
212. Römkens, M.J.M.; Glenn, L.F.; Nelson, D.W.; Roth, C.B. A Laboratory Rainfall Simulator for Infiltration and Soil Detachment Studies1. *Soil Sci. Soc. Am. J.* **1975**, *39*, 158. [\[CrossRef\]](#)

213. Roth, C.H.; Joschko, M. A Note on the Reduction of Runoff from Crusted Soils by Earthworm Burrows and Artificial Channels. *Z. Pflanzenernaehr. Bodenkd.* **1991**, *154*, 101–105. [\[CrossRef\]](#)
214. Schultz, J.P.; Jarrett, A.R.; Hoover, J.R. Detachment and Splash of a Cohesive Soil by Rainfall. *Trans. ASAE* **1985**, *28*, 1878–1884. [\[CrossRef\]](#)
215. Selby, M.J. Design of a Hand-Portable Rainfall-Simulating Infiltrometer, with Trial Results from the Otutira Catchment. *J. Hydrol.* **1970**, *9*, 117–132.
216. Shainberg, I.; Mamedov, A.I.; Levy, G.J. Role of Wetting Rate and Rain Energy in Seal Formation and Erosion 1. *Soil Sci.* **2003**, *168*, 54–62. [\[CrossRef\]](#)
217. Singh, R.; Panigrahy, N.; Philip, G. Modified Rainfall Simulator Infiltrometer for Infiltration, Runoff and Erosion Studies. *Agric. Water Manag.* **1999**, *41*, 167–175. [\[CrossRef\]](#)
218. Summer, R.M. Field and Laboratory Studies on Alpine Soil Erodibility, Southern Rocky Mountains, Colorado. *Earth Surf. Process.* **2007**, *7*, 253–266. [\[CrossRef\]](#)
219. Sutherland, R.A.; Wan, Y.; Ziegler, A.D.; Lee, C.-T.; El-Swaify, S.A. Splash and Wash Dynamics: An Experimental Investigation Using an Oxisol. *Geoderma* **1996**, *69*, 85–103. [\[CrossRef\]](#)
220. Terry, J.P.; Shakesby, R.A. Soil Hydrophobicity Effects on Rainsplash: Simulated Rainfall and Photographic Evidence. *Earth Surf. Process.* **1993**, *18*, 519–525. [\[CrossRef\]](#)
221. Thurow, T.L.; Blackburn, W.H.; Warren, S.D.; Taylor, C.A. Rainfall Interception by Midgrass, Shortgrass, and Live Oak Mottes. *J. Range Manag.* **1987**, *40*, 455. [\[CrossRef\]](#)
222. Tricker, A.S. The Design of a Portable Rainfall Simulator Infiltrometer. *J. Hydrol.* **1979**, *41*, 143–147. [\[CrossRef\]](#)
223. Vahabi, J.; Nikkani, D. Assessing Dominant Factors Affecting Soil Erosion Using a Portable Rainfall Simulator. *Int. J. Sediment Res.* **2008**, *23*, 376–386. [\[CrossRef\]](#)
224. Walker, P.H.; Kinnell, P.I.A.; Green, P. Transport of a Noncohesive Sandy Mixture in Rainfall and Runoff Experiments. *Soil Sci. Soc. Am. J.* **1978**, *42*, 793–801. [\[CrossRef\]](#)
225. Wan, Y.; El-Swaify, S.A.; Sutherland, R.A. Partitioning Interrill Splash and Wash Dynamics: A Novel Laboratory Approach. *Soil Technol.* **1996**, *9*, 55–69. [\[CrossRef\]](#)
226. West, N.E.; Gifford, G.F. Rainfall Interception by Cool-Desert Shrubs. *J. Range Manag.* **1976**, *29*, 171. [\[CrossRef\]](#)
227. Wierda, A.; Veen, A.W.L. A Rainfall Simulator Study of Infiltration into Arable Soils. *Agric. Water Manag.* **1992**, *21*, 119–135. [\[CrossRef\]](#)
228. Will, G.L. Infiltration under a Rainfall Simulator. Master's Thesis, Oregon State University, Corvallis, OR, USA, 1973.
229. Wilson, J.P.; Seney, J.P. Erosional Impact of Hikers, Horses, Motorcycles, and off-Road Bicycles on Mountain Trails in Montana. *Mt. Res. Dev.* **1994**, *14*, 77–88. [\[CrossRef\]](#)
230. Wood, M.K.; Blackburn, W.H. Grazing Systems: Their Influence on Infiltration Rates in the Rolling Plains of Texas. *J. Range Manag.* **1981**, *34*, 331. [\[CrossRef\]](#)
231. Woodburn, R. The Effect of Structural Condition on Soil Detachment by Raindrop Impact. *Agric. Eng.* **1948**, *29*, 154–156.
232. Yamamoto, T.; Anderson, H.W. Splash Erosion Related to Soil Erodibility Indexes and Other Forest Soil Properties in Hawaii. *Water Resour. Res.* **1973**, *9*, 336–345. [\[CrossRef\]](#)
233. Young, R.A. A Method of Measuring Aggregate Stability under Waterdrop Impact. *Trans. ASAE* **1984**, *27*, 1351–1354. [\[CrossRef\]](#)
234. Al-Durrah, M.; Bradford, J.M. New Methods of Studying Soil Detachment Due to Waterdrop Impact. *Soil Sci. Soc. Am. J.* **1981**, *45*, 949–953. [\[CrossRef\]](#)
235. Al-Durrah, M.M.; Bradford, J.M. Parameters for Describing Soil Detachment Due to Single Waterdrop Impact. *Soil Sci. Soc. Am. J.* **1982**, *46*, 836–840. [\[CrossRef\]](#)
236. Al-Durrah, M.M.; Bradford, J.M. The Mechanism of Raindrop Splash on Soil Surfaces. *Soil Sci. Soc. Am. J.* **1982**, *46*, 1086–1090. [\[CrossRef\]](#)
237. Bergsma, E.; Valenzuela, C.R. Drop Testing Aggregate Stability of Some Soils near Merida, Spain. *Earth Surf. Process.* **1981**, *6*, 309–318. [\[CrossRef\]](#)
238. Cruse, R.M.; Larson, W.E. Effect of Soil Shear Strength on Soil Detachment Due to Raindrop Impact1. *Soil Sci. Soc. Am. J.* **1977**, *41*, 777. [\[CrossRef\]](#)
239. Farres, P.J.; Cousen, S.M. An Improved Method of Aggregate Stability Measurement. *Earth Surf. Process.* **1985**, *10*, 321–329. [\[CrossRef\]](#)
240. Francis, P.B.; Cruse, R.M. Soil Water Matric Potential Effects on Aggregate Stability. *Soil Sci. Soc. Am. J.* **1983**, *47*, 578–581. [\[CrossRef\]](#)
241. Furbish, D.J.; Hamner, K.K.; Schmeckle, M.; Borosund, M.N.; Mudd, S.M. Rain Splash of Dry Sand Revealed by High-Speed Imaging and Sticky Paper Splash Targets. *J. Geophys. Res.* **2007**, *112*. [\[CrossRef\]](#)
242. Ghadir, H.; Payne, D. The Formation and Characteristics of Splash Following Raindrop Impact on Soil. *J. Soil Sci.* **1988**, *39*, 563–575. [\[CrossRef\]](#)
243. Hobbs, P.V.; Osheroff, T. Splashing of Drops on Shallow Liquids. *Science* **1967**, *158*, 1184–1186. [\[CrossRef\]](#)
244. Lane, W.R. A Microburette for Producing Small Liquid Drops of Known Size. *J. Sci. Instrum.* **1947**, *24*, 98–101. [\[CrossRef\]](#)
245. Magono, C. On the Shape of Water Drops Falling in Stagnant Air. *J. Meteorol.* **1954**, *11*, 77–79. [\[CrossRef\]](#)

246. Mutchler, C.K. Using the Drift of Waterdrops during Fall for Rainfall Simulator Design. *J. Geophys. Res.* **1965**, *70*, 3899–3902. [[CrossRef](#)]
247. Mutchler, C.K.; Hansen, L.M. Splash of a Waterdrop at Terminal Velocity. *Science* **1970**, *169*, 1311–1312. [[CrossRef](#)]
248. Mutchler, C.K.; Larson, C.L. Splash Amounts from Waterdrop Impact on a Smooth Surface. *Water Resour. Res.* **1971**, *7*, 195–200. [[CrossRef](#)]
249. Nearing, M.A.; Bradford, J.M. Single Waterdrop Splash Detachment and Mechanical Properties of Soils. *Soil Sci. Soc. Am. J.* **1985**, *49*, 547–552. [[CrossRef](#)]
250. Palmer, R.S. The Influence of a Thin Water Layer on Waterdrop Impact Forces. *Int. Assoc. Sci. Hydrol. Publ.* **1963**, *65*, 141–148.
251. Palmer, R.S. *An Apparatus for Forming Waterdrops*; U.S. Department of Agriculture: Washington, DC, USA, 1962; Volume 61.
252. Palmer, R.S. Waterdrop Impact Forces. *Trans. ASAE* **1965**, *8*, 69–70. [[CrossRef](#)]
253. Ryan, R.T. The Behavior of Large, Low-Surface-Tension Water Drops Falling at Terminal Velocity in Air. *J. Appl. Meteorol.* **1976**, *15*, 157–165. [[CrossRef](#)]
254. Ryżak, M.; Bieganski, A. Using the Image Analysis Method for Describing Soil Detachment by a Single Water Drop Impact. *Sensors* **2012**, *12*, 11527–11543. [[CrossRef](#)]
255. Ryżak, M.; Bieganski, A.; Polakowski, C. Effect of Soil Moisture Content on the Splash Phenomenon Reproducibility. *PLoS ONE* **2015**, *10*, e0119269. [[CrossRef](#)]
256. Savat, J. Work Done by Splash: Laboratory Experiments. *Earth Surf. Process.* **1981**, *6*, 275–283. [[CrossRef](#)]
257. Sharma, P.P.; Gupta, S.C.; Rawls, W.J. Soil Detachment by Single Raindrops of Varying Kinetic Energy. *Soil Sci. Soc. Am. J.* **1991**, *55*, 301. [[CrossRef](#)]
258. Yu, C.-K.; Hsieh, P.-R.; Yuter, S.E.; Cheng, L.-W.; Tsai, C.-L.; Lin, C.-Y.; Chen, Y. Measuring Droplet Fall Speed with a High-Speed Camera: Indoor Accuracy and Potential Outdoor Applications. *Atmos. Meas. Tech.* **2016**, *9*, 1755–1766. [[CrossRef](#)]
259. Israelsen, C.E.; Israelsen, E.K.; Fletcher, J.E.; Fifield, J.S.; Canfield, R.V. *Erosion Control Product Testing*. 1979. Available online: https://digitalcommons.usu.edu/water_rep/367/ (accessed on 12 October 2022).
260. Roth, C.H.; Helming, K. Dynamics of Surface Sealing, Runoff Formation and Interrill Soil Loss as Related to Rainfall Intensity, Microrelief and Slope. *Z. Für Pflanz. Und Bodenkd.* **1992**, *155*, 209–216. [[CrossRef](#)]
261. Bombino, G.; Denisi, P.; Gómez, J.; Zema, D. Water Infiltration and Surface Runoff in Steep Clayey Soils of Olive Groves under Different Management Practices. *Water* **2019**, *11*, 240. [[CrossRef](#)]

Disclaimer/Publisher’s Note: The statements, opinions and data contained in all publications are solely those of the individual author(s) and contributor(s) and not of MDPI and/or the editor(s). MDPI and/or the editor(s) disclaim responsibility for any injury to people or property resulting from any ideas, methods, instructions or products referred to in the content.